Multi-objective Short-Term Scheduling of a Renewable-based Microgrid in the Presence of Tidal Resources and Storage Devices

Mahshid Javidsharifi[a], Taher Niknam[a*], Jamshid Aghaei[a] and Geev Mokryani[b]

a. Department of Electrical Engineering, Shiraz University of Technology, Shiraz 71555-313, Iran

b. School of Electrical Engineering and Computer Science, University of Bradford, Bradford BD7 1DP, UK

m.javidsharifi@sutech.ac.ir, niknam@sutech.ac.ir, aghaei@sutech.ac.ir, g.mokryani@bradford.ac.uk

Abstract-Daily increasing use of tidal power generation proves its outstanding features as a renewable source. Due to environmental concerns, tidal current energy which has no greenhouse emission attracted researchers' attention in the last decade. Additionally, the significant potential of tidal technologies to economically benefit the utility in long-term periods is substantial. Tidal energy can be highly forecasted based on short-time given data and hence it will be a reliable renewable resource which can be fitted into power systems. In this paper, investigations of effects of a practical stream tidal turbine in Lake Saroma in the eastern area of Hokkaido, Japan, allocated in a real microgrid (MG), is considered in order to solve an environmental/economic bi-objective optimization problem. For this purpose, an intelligent evolutionary multi-objective modified bird mating optimizer (MMOBMO) algorithm is proposed. Additionally, a detailed economic model of storage device is considered in the problem. Results show the efficiency of the suggested algorithm in satisfying economic/environmental objectives. The effectiveness of the proposed approach is validated by making comparison with original BMO and PSO on a practical MG.

***Index Terms*— tidal energy, microgrid, environmental/economic optimization, renewable energy sources, storage devices, modified bird mating optimizer algorithm.**

1. Introduction

Tides, i.e. ocean water oscillations, occur due to gravity principles among the moon, the sun and the earth. Therefore, tidal energy can be assumed as a class of renewable energies. In comparison with other kinds of renewable resources such as wind and solar, tidal energy can be claimed to be better predictable according to the short time data categories [1]. With the possibility of acquiring accurate tidal prediction, researchers can rely confidently on tidal currents to produce electricity for long term periods [2]. From the emission standpoint, tidal energy does not result in any air, water or thermal pollution. However, from the economic standpoint, although the primary investment of tidal power is approximately high, its subsequent benefits are highly considerable. Tidal energy technologies are categorized into three major groups, namely tidal range, tidal current or tidal stream turbines (TST) and hybrid technologies [2].

Inadequate amounts of fossil fuel along with global warming concerns give rise to the appearance of renewable energy sources (RES) among which tidal turbines are of great importance according to the above mentioned advantages. Different RESs including tidal, photovoltaic (PV) and wind generators beside energy storage systems are used in microgrids (MGs) in order to take their benefits as power generators to increase the reliability of the power system and to yield better performance [3]. In order to supply the load while minimum levels of cost and emission are satisfied under considered constraints, the economic\environmental dispatch of MGs shall be taken into account as a multi-objective problem.

The choice of optimization techniques for solving multi-objective problems depends on several different factors. Consequently, diverse methods including mathematical programming-based optimization approaches and meta-heuristic algorithms can be proposed [4-6]. The lambda iterative method, gradient projection method, Lagrange relaxation, linear/non-linear programming interior point methods, dynamic programming, etc. are examples of mathematical programming-based methods. Authors of [7] introduce a multi-objective Mixed Integer Linear Programming (MILP) approach for MG energy management problems. However, some other researchers have proposed meta-heuristic methods in order to deal with MG operation problems. The main reason and motivation for applying meta-heuristic algorithms over mathematical programming-

based optimization approaches in order to solve multi-objective problems is that the former deals simultaneously with a set of feasible solutions which allows to find different solutions in the Pareto optimal front with executing the algorithm only once, rather than using a sequence of independent executions as is done in mathematical programming. Additionally, meta-heuristic algorithms are not sensitive to the continuity and formation of the Pareto front, which is one of the drawbacks of mathematical programming. Four of the main scopes of meta-heuristic algorithms in multi-objective problems are: i) maintaining the non-dominated solutions, ii) conducting the present Pareto front to an optimal one, iii) generating the Pareto optimal front and maintaining their diversity, and iv) presenting a decision-making procedure to select a limited number of Pareto optimal solutions.

In order to investigate the day-ahead scheduling of a MG, several multi-objective models have been proposed [8-26]. The proposed model in [8] considered both energy cost and the thermal comfort of MG resources. Minimizing the emissions is surveyed in most of the proposed multi-objective models for short-term MG energy management problem [9-14]. Some papers investigate the multi-objective optimal operation of MGs, applying different meta-heuristic algorithms [9-22]. A multi-objective mesh-adaptive direct search is presented in [9] to minimize the total cost in order to optimize the environmental economic problem in MG. A Teaching-Learning Based Optimization (TLBO) algorithm is used in [10] for solving multi-objective optimal operation of MG, while authors in [11] have presented a θ-krill herd algorithm to solve the problem. A modified Bacterial Foraging Optimization algorithm is proposed in [12 & 13] for optimal operation of a Combined Heat and Power-based (CHP-based) MG over a 24-hour time interval. Moghaddam et al. proposed an Adaptive Modified Particle Swarm Optimization (AMPSO) algorithm in [4]. A θ-PSO algorithm is applied in [14] to solve the MG's energy management problem. A Multi-Cross Learning-Based Chaotic Differential Evolution (MLCDE) algorithm is proposed in [15] for optimal operation management of an islanded MG. A Multi-objective PSO algorithm is used in [16] in order to optimize the MG's short-term performance. Soares et al. [17] proposed a Signaled Particle Swarm Optimization (SiPSO) for MG scheduling. Using a hybrid harmony search algorithm with differential evolution, day-ahead scheduling problem of an MG is considered in [18]. A Real-Time Energy Management System (RT-EMS) is introduced to take advantage of Genetic Algorithm (GA) for minimizing energy cost beside carbon dioxide emissions while maximizing the power of available RESs [19]. Marzband et al. scrutinize the optimal operation scheduling of MGs using a gravitational search algorithm while fulfilling technical constraints [20]. A two-stage optimization method is presented in [21] which applies PSO along with a deterministic technique based on MILP for the daily operation of a smart grid. A multi-objective model-based optimization method is expressed in [22] for optimal sizing of all components and determination of the power electronic layout. In order to minimize economic and environmental objectives, the main problem is divided into three optimization problems. The Multi-objective Ant Lion Optimizer (MOALO) is applied in [23] and a two-stage optimization method is proposed in order to maximize the investment benefits and system voltage stability and to minimize line losses. In [24] a Mixed-integer Programming (MIP) is used in order to solve a multi-objective self-scheduling optimization problem. Artificial intelligence techniques jointly with linear-programming-based multi-objective optimization is presented in [25] for intelligent energy management of a MG. An improved real-coded genetic algorithm and an enhanced MILP based method is suggested in [26] to schedule the unit commitment and economic dispatch of MG units.

On the other hand, some researches are devoted to the structure and operational performance of tidal devices [27-29], while some others basically focus on reliability evaluation of tidal power generation systems [30 & 31]. However, to the best of the authors' knowledge, energy management of MGs including tidal turbines while considering the exact model of battery along with the tidal turbine economic/environmental modelling has not been contemplated in the literature. Consequently, in this paper in order to investigate an MG's environmental/economic bi-objective optimization problem, the Modified Multi-Objective Bird

Mating Optimizer (MMOBMO) algorithm is proposed. The Bird Mating Optimizer (BMO) algorithm which, has a simple concept and is easy to implement, was first suggested by Askarzadeh [32] in 2014. It is worth mentioning that BMO benefits from all proper features of such algorithms as GA and DE. Besides, since five different societies of birds are defined in this algorithm, it is capable of exploring the search space effectively while exploiting the best found regions. These aspects make BMO an approximately precise algorithm which is less probable to be trapped in local optima [32]. Hence, to take all advantages of BMO while improving its search speed and precision, the MMOBMO algorithm is presented in this paper. The present paper attempts to improve the weaknesses of the applied optimization algorithms considered in the literature for solving MGs optimal operation management and deal with different scopes of network operation. Consequently, the main contributions of the paper can be summarized as:

1. The proposed MMOBMO algorithm is able to appropriately deal with multi-objective energy management of MGs, while considering different - sometimes conflicting - objectives.
2. The economic/environmental modelling of the practical TST of the Lake Saroma green microgrid (SLMG) [33] is studied while the data of a real MG are examined. It was observed that since PV and tidal generators are complementary, an MG consisting of these two generators is more proper in sustainably supplying the loads.
3. The introduced optimal scheduling intents on minimizing the total cost of day-ahead market transactions and fuel costs, while it also aims at minimizing emission of MG.
4. The proposed scheme also concentrates on the reduction of MG's dependency on the main grid and the electricity market as well as on maximizing the utilization of RESs in the considered region.
5. A new model of the storage device (i.e. Li-ion battery in this paper) in order to consider the battery power constraints along with the battery state of charge (SOC) is presented. The influence of the existence of storage devices on the MG's energy management is observed through simulation results.
6. Since the On and Off states of DGs are taken into account, a mixed-integer problem is solved in the article using the novel MMOBMO algorithm which involves all of the advantages of the original BMO while the convergence capability and speed of the algorithm are improved.
7. An efficient method is applied to control the size of the repository of Pareto solutions which leads to having a well-distributed Pareto optimal front. Compared to PSO and the original BMO, the proposed method demonstrates fast convergence and very low computational time as well as better solutions. The robustness of the algorithm, as another outstanding feature, is highlighted through the simulation results.
8. In order to satisfy the power balance equality constraint, a new approach is presented based on the correction method using which better solutions are achieved faster than those of the penalty factor procedure.

The remainder of this paper is as follows: in Section 2 tidal energy technologies are introduced and the economic/environmental modelling of TSTs is presented. In Section 3 the problem is formulated and objective functions along with the constraints are presented. In Section 4 Fundamentals of multi-objective problems and a presentation of the proposed algorithm are discussed; additionally, the applied methodology for solving the optimal operation management problem in an ordinary MG is explained. Results are investigated in Section 5. Finally, conclusions are highlighted in Section 6.

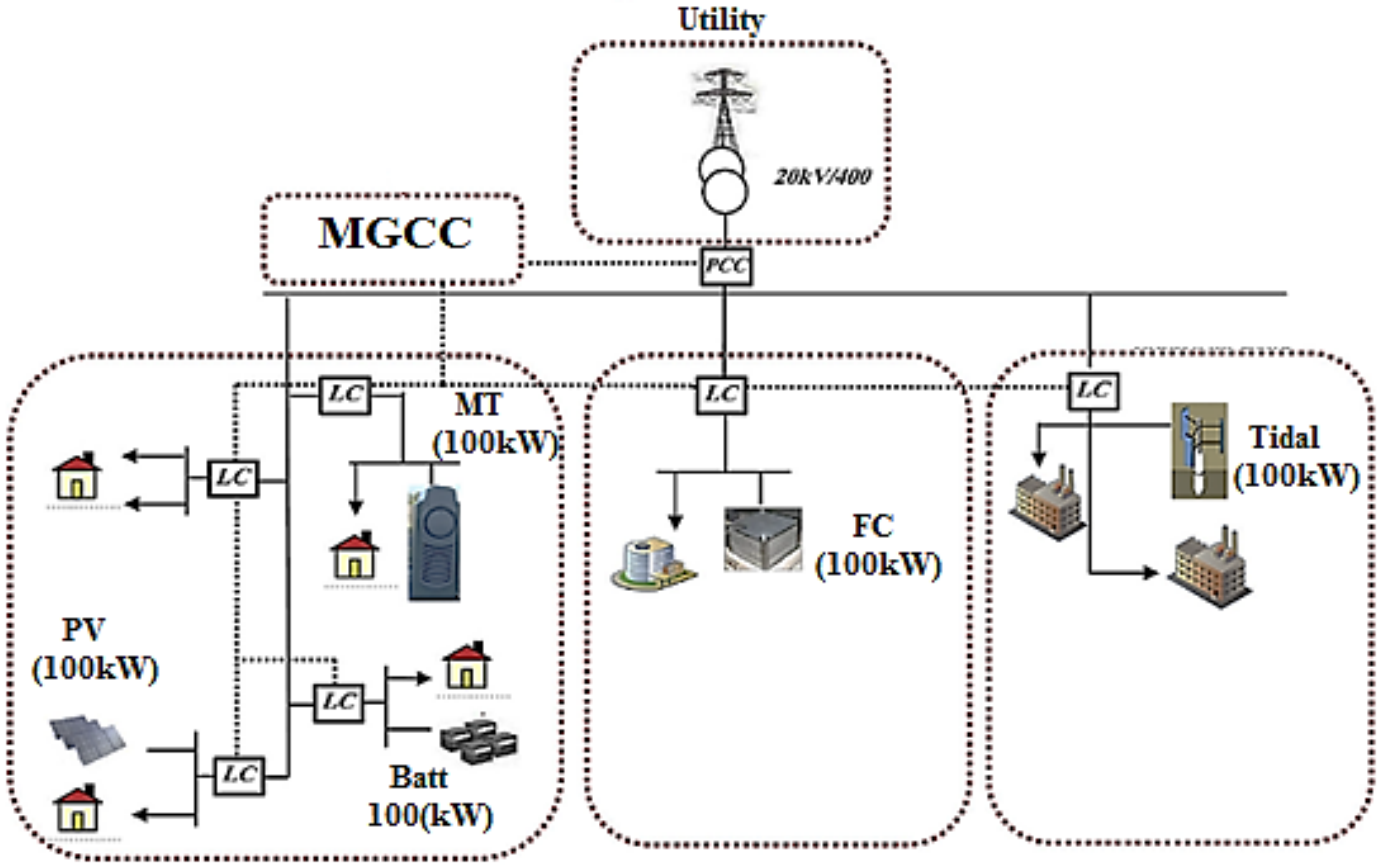

Fig.1. Renewable MG including TST, PV, FC, MT and storage device.

2. Economic/Environmental Modeling of Tidal Stream Generators

2.1. Tidal Energy Technologies

Although there are few economically practical sites in the world which utilize tidal energy, in order to meet future needs of local electricity generation, harnessing energy from tidal currents has been gaining remarkable attention [34]. Challenges focus on different technologies and developments of the prototypes. Two main factors to be considered in the tidal turbines' structures are persistence against natural disasters such as storms and high waves, besides minimizing the possible impacts on the environment and marine life while producing efficient electricity [35]. Accordingly, there are three categories of tidal energy technologies which are explained in the following.

For the first time, tidal range/barrage technology was installed in La Rance, France in 1960s as the most common technology [36]. The construction can generate electricity with ebb, flood tides or both using a one- or bi-directional turbine structure. The power generation occurs when the difference in the water height reaches an even level on both sides of the barrage. The ebb and flood tides create the potential energy which can be used for generation of electricity by tidal generators. The function of ebb-based one directional turbines is illustrated in Fig. 2. It should be mentioned that due to the heavy capital costs and harmful effects on regional ecosystems, e.g. sea life, navigation and birds' life, this type of tidal energy utilization is not much considerable nowadays. Another deficiency of tidal barrage technologies is that they are merely able to harvest power for 10 hours each day [37].

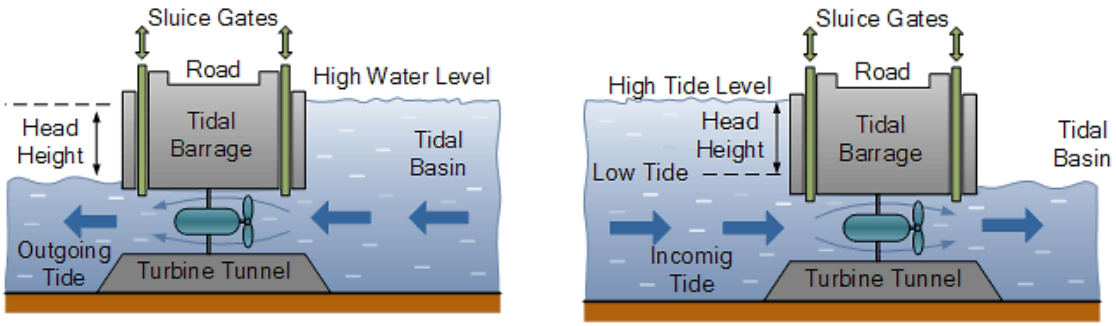

Fig. 2. The function of tidal barrage technology.

The second common technology is tidal stream turbines (TST) which are basically very similar to wind turbines. Owing to the fact that TSTs are physically smaller and have lower visual impact as a result of the fact that most of the device is submerged under water, they are more preferable compared to on- or off-shore wind turbines. TSTs are submerged in the shallow sea water and rotate very slowly without need for barrage or dam buildings; therefore, they do not manipulate the ecosystem and have essentially environmentally friendly structures [36]. This technology substantially converts the kinetic energy of the water to electrical energy according to the tides motions. The turbine extracts the kinetic energy of the water and converts it to electricity by the generator [36 & 37]. A complete review on different types of turbines used in this technology is included in [38].

Some forms of tidal range technologies have great potential to be combined with planning and design of new infrastructure for coastal zones from design and arrangement points of view [37]. These multi-purpose technologies, namely hybrid generators, take advantage from both tidal range and stream generators in the process of production of electricity. Additionally, a hybrid form of tidal range and current power generation, namely dynamic tidal power, is also toward improvement. However, no full-scale prototype has been yet tested or demonstrated [37].

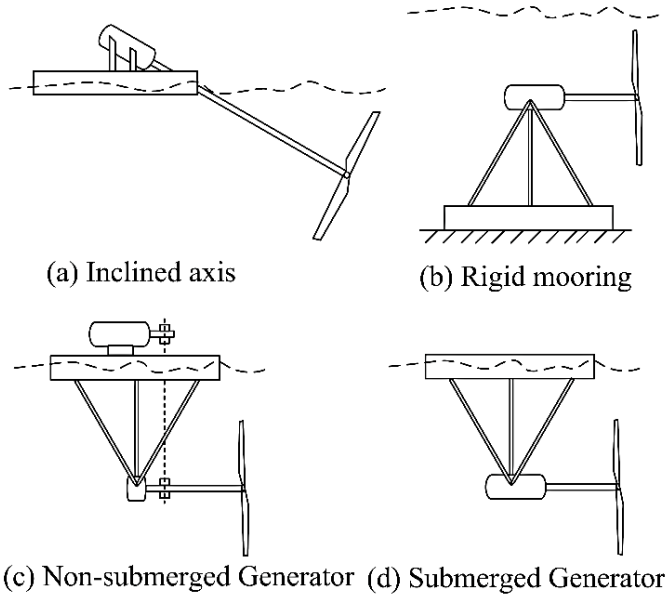

Fig. 3. Horizental axis turbines.

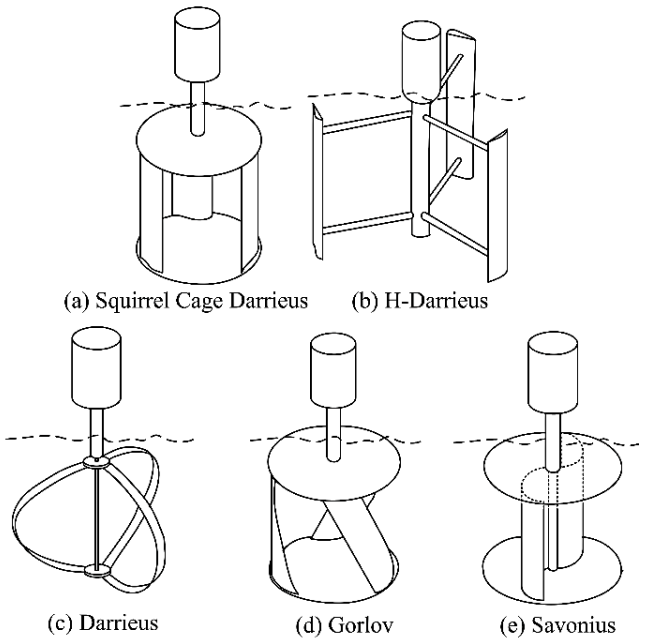

Fig. 4. Vertical axis turbines.

2.2. Power output model of TST

Due to the fact that TSTs circulate slowly under water and do not need a barrage or dam in the structure, they are the most promising technology which do not involve the environmental drawbacks of barrages [37]. The applied turbines in this technology are categorized into three groups: horizontal axis, vertical axis and enclosed [38]. Ducted or shrouded turbines are included in the first group. The second category is comprised of reciprocating devices. Other implemented designs such as rotating screw-like devices and tidal kites can be put in the third category [30]. Some examples of different horizontal and vertical axis turbines are shown in figures 3 and 4. In the considered MG, tidal currents were converted into electrical energy via a three-phase synchronized generator connected to Darrieus water turbines [33].

The kinetic energy of a tidal current is driven based on its speed as follows:

$$E = \frac{1}{2}.m.V^2 \ , \quad m = \rho.A.V \tag{1}$$

where ρ is the water density (kg/m^3), A is the cross section of the turbine (m^2) and V is the water velocity (m/s). However, similar to wind turbines, only a fraction of the available kinetic energy can be extracted [39]:

$$P_{TST} = N \times \eta \times \mu \times \frac{1}{2} \times \rho \times A \times V^3 \tag{2}$$

where N is the number of turbines at the site, η is the turbine efficiency (35%) and μ is the theoretical extractable power affected by the bottom drag and the ability of the water to stream around the turbine.

When the cut-in speed and the rated speed are considered as V_{cutin} and V_{rated}, the output power of a TST (P_{out}) is calculated as follows [30]:

$$P_{out} = \begin{cases} 0 & 0 < V < V_{cutin} \\ \frac{1}{2} C_P \rho A V^3 & V_{cutin} \le V < V_{rated} \\ P_{rated} & V_{rated} \le V \end{cases} \tag{3}$$

where P_{rated} is the rated power, C_p is the power capture coefficient the value of which is in the range of 0.4~0.5. Accordingly, the speed-power characteristic of a TST can be illustrated as by Fig. 5.

Fig. 6 demonstrates tidal current velocities during the whole 24 hours of a specific day (August 5th) for Lake Saroma. Negative velocities represent flood tides, while positive velocities are representative of ebbing tides [33].

2.3. Environmental Considerations

Modelling of tidal turbine is investigated from two points of view, including emission and economic. Renewable energies can help to displace a considerable amount of CO_2 emission. Being a renewable energy source, tidal generators do not produce any emission. Consequently, in the emission objective function no term exists to indicate tidal emission.

2.4. Economic Modelling

Depending on the turbine size and water velocity, a relatively small amount of power ranging from 25 kW to 250 kW can be driven from the TSTs. In order to produce a power level equal to that of conventional power plants, turbines can be used in groups [40]. Since the density of water is 832 times that of air, TSTs are able to extract more energy at lower velocities.

Consequently, TSTs will produce forty times more power compared to a windmill of similar size. According to [36], the levelized cost of energy (*LCOE*) for TSTs is in the range of 0.25-0.47 EUR/kWh. The economic modelling of TSTs which is considered in this research is as follows:

$$Cost = LCOE \times P_{TST} \tag{4}$$

where P_{TST} represents the output power of TST, and *LCOE* is the levelized cost of energy which includes investment, operation and maintenance costs. The levelized cost can be calculated through two methods, namely "discounting" and "annuitizing," which are explained in [41] in details.

From the characteristics of Lake Saroma mentioned in [33] and using equations (3) and (4), the economic model of the system under study can be estimated.

In the economic/environmental dispatch of the considered MG (Fig. 1.), the On\Off states of the distributed generator (DG) units along with the optimal allocation of power generation set points are defined such that the objective functions, that include the operating cost and emission of the MG, are minimized whilst several constraints are satisfied [14].

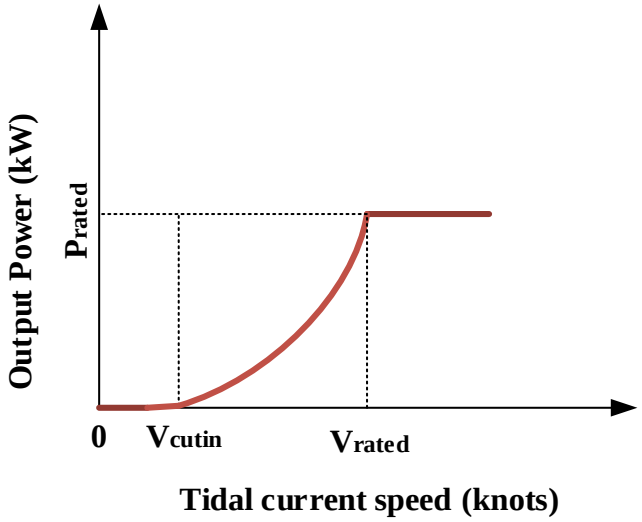

Fig. 5. Speed-power characteristic of TST [30].

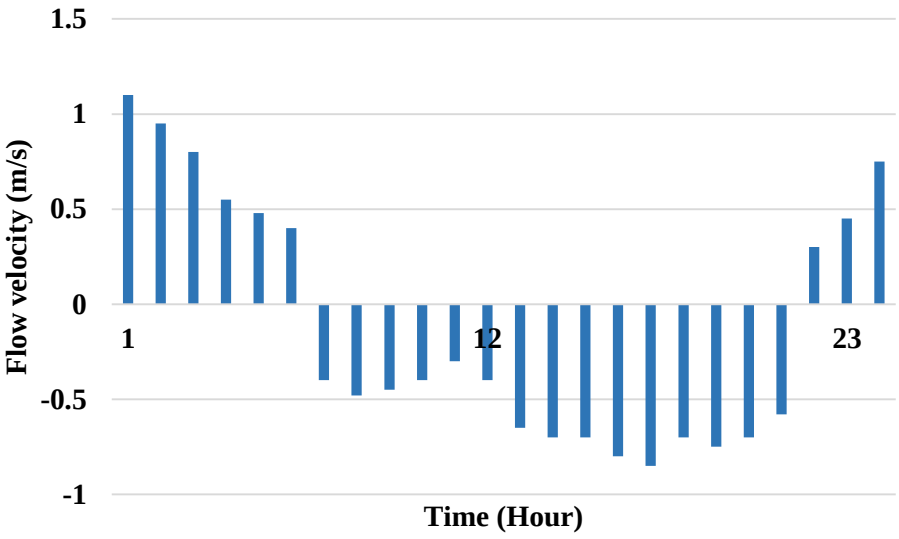

Fig. 6. Tidal current velocity in a specific day [33].

3. Problem formulation

3.1. Cost and Emission Minimization

As the first objective function, the total operation cost should be minimized as follows [42]:

$$F_1(\overset{\rho}{X}) = \sum_{t=1}^{T} Cost^t = \sum_{t=1}^{T} \left\{ \sum_{i=1}^{N_{DG}} [u_i^t.(P_{DGi}^t).B_{DGi}^t + SUC_{DGi}.u_i^t.(1-u_i^{t-1}) + SDC_{DGi}.u_i^{t-1}.(1-u_i^t)] + \sum_{r=1}^{N_{RES}} [P_{RES_r}^t.B_{RES_r}^t] + \sum_{s=1}^{N_{Batt}} [P_{Batt_s}^t.B_{Batt_s}^t + Cost_{Deg_s}^t] + P_{Grid}^t.B_{Grid}^t \right\} \quad (5)$$

$$\overset{\nu}{X} = \left[\overset{\nu}{U}_{DG}, \overset{\nu}{P}_{DG}, \overset{\nu}{P}_{Batt}, \overset{\nu}{P}_{Grid}\right]_{1\times n} \quad (6a)$$

$$n = [((2\times N_{DG}) + N_{Batt}) + 1]\times T$$

$$\overset{\nu}{U}_{DG} = \left[\overset{\rho}{u}_1, \overset{\rho}{u}_2, \ldots, \overset{\rho}{u}_{N_{DG}}\right] = \{\overset{\rho}{u}_i\}_{1\times N_{DG}} \in \{0,1\} \quad (6b)$$

$$\overset{\rho}{u}_i = \left\{u_i^1, u_i^2, \ldots, u_i^t, \ldots, u_i^T\right\} \quad i = 1,2,\ldots,N_{DG} \quad (6c)$$

$$\overset{\nu}{P}_{DG} = \left\lfloor \overset{\nu}{P}_{DG_1}, \overset{\nu}{P}_{DG_2}, \ldots, \overset{\nu}{P}_{DG_{N_{DG}}} \right\rfloor \quad (6d)$$

$$\overset{\nu}{P}_{DGi} = \left\{P_{DGi}^1, P_{DGi}^2, \ldots, P_{DGi}^t, \ldots, PD_{Gi}^T\right\} \quad i = 1,2,\ldots,N_{DG} \quad (6e)$$

$$\overset{\nu}{P}_{Batt} = \left\lfloor \overset{\nu}{P}_{Batt_1}, \overset{\nu}{P}_{Batt_2}, \ldots, \overset{\nu}{P}_{Batt_{N_{Batt}}} \right\rfloor \quad (6f)$$

$$\overset{\nu}{P}_{Batt,s} = \left\{P_{Batt,s}^1, P_{Batt,s}^2, \ldots, P_{Batt,s}^t, \ldots, P_{Batt,s}^T\right\} s = 1,2,\ldots,N_{Batt} \quad (6g)$$

$$\overset{\nu}{P}_{RES} = \left\lfloor \overset{\nu}{P}_{RES_1}, \overset{\nu}{P}_{RES_2}, \ldots, \overset{\nu}{P}_{RES_{N_{RES}}} \right\rfloor$$

(6h)

$$\vec{P}_{RES_r} = \left[P^1_{RES_r}, P^2_{RES_r}, \ldots, P^t_{RES_r}, \ldots, P^T_{RES_r}\right]; r = 1,2,\ldots,N_{RES} \quad (6i)$$

$$\vec{P}_{Grid} = \left[P^1_{Grid}, P^2_{Grid}, \ldots, P^t_{Grid}, \ldots, P^T_{Grid}\right] \quad (6j)$$

where $Cost^t$ is the MG's operation cost in hour *t*. $\vec{X}$ is the vector of design variables, and *n* is the number of design variables. *T* is the total number of hours. The total number of dispatchable generations and storage units (battery) along with the number of RESs are N_{DG}, N_{Batt} and N_{RES}, respectively. It should be mentioned that *DG* demonstrates the dispatchable units including fuel cell (FC) and micro-turbine (MT), while *Grid* and *Batt* represent the utility grid and the battery, respectively. The TST and PV are shown with *RES* as non-dispatchable units. Note that the utility has to buy all of the electrical power produced by RES units; consequently, RESs' output powers ($P^t_{RES,r}$) are not included in the design variables' vector. u^t_i is applied to imply the ON or OFF states of the i^{th} dispatchable DG during each hour of the day. P^t_{DGi}, $P^t_{RES_r}$ and $P^t_{Batt,s}$ represent the real output powers (kWh) of the i^{th} DG, r^{th} RES and s^{th} storage at time *t*, respectively. The active power which is bought (sold) from (to) the utility at time *t* is demonstrated by P^t_{Grid}. B^t_{DGi}, $B^t_{RES_r}$, $B^t_{Batt,s}$ and B^t_{Grid} are respectively bids of dispatchable DGs, RESs, storage devices and the utility grid at hour *t* (€/kWh). SUC_{DGi} and SDC_{DGi} are the start-up and shut-down costs for the i^{th} dispatchable DG. $(P^t_{DGi}.B^t_{DGi})$, $(P^t_{RES_r}.B^t_{RES_r})$, $(P^t_{Batt_s}.B^t_{Batt_s})$ and $(P^t_{Grid}.B^t_{Grid})$ represent operational costs of dispatchable DGs, RESs, battery and the cost of power exchange between the MG and utility (€), respectively. $Cost^t_{Deg}$ is the battery degradation cost which is achieved as follows [47]:

$$Cost^t_{Deg} = \frac{C_{Batt}.DoD.E_{Batt}}{N_{cycle}} \quad (7)$$

where C_{Batt} is the investment cost of the battery while E_{Batt} is the usable energy of the battery. DoD indicates an absolute discharge relative to the rated battery capacity. Literally, DoD is a function of the SOC of a battery which is defined as the ratio of its current capacity ($Q(t)$) to the nominal capacity (Q_n), $(SOC(t) = \frac{Q(t)}{Q_n}).Q_n$ is representative of the maximum amount of charge that can be stored in the battery and is given by the manufacturer [44]. In this paper the following is applied to show the DoD of the battery [43]:

$$DoD = \frac{E_{Batt,\max} - E_i}{E_{Batt,\max}} \quad (8)$$

where $E_{Batt,\max}$ is the maximum energy stored in the battery and E_i is the energy stored in the battery at a specific hour of the day. The cycle life of the battery is then achieved as follows:

$$N_{cycle} = a.DoD^b \quad (9)$$

where *a* and *b* are battery-specific parameters which are for example 1331 and -1.825, respectively, for a Li-ion battery [43].

The second objective is minimization of the environmental pollutants. Three different pollutants are considered in the objective function as in the following [45]:

$$F_2(\vec{X}) = \sum_{t=1}^{T} Emission^t = \sum_{t=1}^{T} \left\{ \sum_{i=1}^{N_{DG}} [u_i^t . (P_{DGi}^t) . E_{Gi}^t] + \sum_{s=1}^{N_{Batt}} [P_{Batt_s}^t . E_{Batt_s}^t] + P_{Grid}^t . E_{Grid}^t \right\} \quad (10)$$

where $Emission^t$ is the amount of produced pollutants emission in one hour of MG's operation. $E_{DGi}^t, E_{Batt_s}^t$ and E_{Grid}^t are the amounts of pollutants emission (kg/kWh) for each generator, storage device and utility at hour *t*, respectively. These variables are described as follows [42]:

$$\begin{aligned} E_{DGi}^t &= CO_{2_{DG_i}}^t + SO_{2_{DG_i}}^t + NO_{x_{DG_i}}^t \\ E_{si}^t &= CO_{2_{Batt,s}}^t + SO_{2_{Batt,s}}^t + NO_{x_{Batt,s}}^t \\ E_{Grid}^t &= CO_{2_{Grid}}^t + SO_{2_{Grid}}^t + NO_{x_{Grid}}^t \end{aligned} \quad (11)$$

where $CO_{2_{DG_i}}^t$, $SO_{2_{DG_i}}^t$ and $NO_{x_{DG_i}}^t$ are the amounts of CO_2, SO_2 and NO_x emission from the i^{th} DG source at hour *t*; $CO_{2_{Batt,s}}^t$, $SO_{2_{Batt,s}}^t$ and $NO_{x_{Batt,si}}^t$ are the amounts of CO_2, SO_2 and NO_x emission from the s^{th} storage unit at hour *t* of the day, and $CO_{2_{Grid}}^t$, $SO_{2_{Grid}}^t$ and $NO_{x_{Grid}}^t$ are the amounts of CO_2, SO_2 and NO_x emission from the utility at hour *t*, respectively.

3.2. Constraints

The balance of electricity demand and supply is one of the most important requirements in MG management [42], hence:

$$\sum_{i=1}^{N_{DG}} [u_i^t . P_{DGi}^t] + \sum_{r=1}^{N_{RES}} [P_{RES_r}^t] + \sum_{s=1}^{N_{Batt}} [P_{Batt_s}^t] + P_{Grid}^t = P_{LD}^t \quad (12)$$

where P_{LD}^t is the total MG load at hour *t*.

In order to consider the limitation on charge and discharge rates of the storage devices during each time intervals, along with limits on the SOC of each storage device are the following equation and constraints mentioned for a typical battery [45]:

$$P_{ch}^t \le P_{ch,\max};\ P_{disch}^t \le P_{disch,\max} \quad (13)$$

The SOC should not violate a pre-determined maximum or minimum value [45]:

$$SOC_{\min} \le SOC_t \le SOC_{\max} \quad (14)$$

Power generations for each dispatchable DG are limited as:

$$u_i^t . P_{DG_{i,\min}}^t \le P_{DG_i}^t \le u_i^t . P_{DG_{i,\max}}^t \quad (15)$$

The power exchange with utility grid is constrained as follows:

$$P_{Grid,\min}^t \le P_{Grid}^t \le P_{Grid,\max}^t \quad (16)$$

Constraints on the rate of charge and discharge of the battery during an hour are considered as the following:

$$P_{Batt_s,\min}^t \le P_{Batt_s}^t \le P_{Batt_s,\max}^t \quad (17)$$

4. Application of the Proposed Methodology

4.1. Multi-Objective Optimization

In a typical multi-objective problem, a number of conflict objective functions are simultaneously optimized. In most cases, multi-objective problems have more than one optimal solution, which are called non-dominated solutions. The obtained non-dominated solutions will be saved in a repository. Within the whole search space, the non-dominated solutions are expressed as Pareto-optimal which establish the Pareto-optimal set or Pareto-optimal front [46 & 47].

The achieved Pareto optimal solutions are excessive, and may lead to a time consuming process. However, since the size of the repository is limited, a finite number of solutions can be stored. Consequently, the size of the repository should be controlled in an efficient way. Accordingly, in this paper, when the number of non-dominated solutions in the repository exceeds a predefined value, namely N_{bound}, they are sorted in an ascending manner according to one of the objective functions, and the first and the last sorted non-dominated solutions are assumed as *A* and *Z*, respectively. The Pareto optimal front is then divided into several intersections according to the following:

$$epsilon = \frac{\sqrt{\sum_{m=1}^{M} (f_{A_m} - f_{B_m})^2}}{N_{bound}} \tag{18}$$

where *M* is the number of objective functions.

For each non-dominated solution in the Pareto front, the distance between the particle and *A* is calculated as follows:

$$distance = \sqrt{\sum_{m=1}^{M} (f_{1_m} - f_{i_m})^2} \tag{19}$$

where f_i is the objective function. Comparing the *epsilon* and *distance* of each particle, non-dominated solutions in each intersection are found. Among the solutions found in each intersection, the one with the maximum distance is considered as the solution which should be stored in the repository. It should be mentioned that according to the limitation of the repository size, the proposed approach also results in appropriate dispersion of optimal Pareto front solutions.

Considering each objective function to be minimized independently, the best solution of each should be obtained. Consequently, particles must be avoided to accumulate in the populated domains. Hence, the proposed method of [48] is applied to select the global best compromised solution. In this technique, the objective functions are normalized such that relatively equal significance is provided to both objectives as follows:

$$Min\phi^M = \omega_1 \left[\frac{\sum_{i=1}^{N_{non-dom}} f_{1_i} - f_1^{\min}}{f_1^{\max} - f_1^{\min}} \right] + \omega_2 \left[\frac{\sum_{i=1}^{N_{non-dom}} f_{2_i} - f_2^{\min}}{f_2^{\max} - f_2^{\min}} \right] \tag{20}$$

where f_1 and f_2 are cost and emission objective functions, respectively. The initial guess for ω_1 and ω_2 is equal to 0.5.

4.2. Modified BMO Algorithm

4.2.1. Bird Mating Optimizer Algorithm

A population-based evolutionary algorithm, namely Bird Mating Optimizer (BMO), was presented by Askarzadeh [32]. The algorithm is impressed by the social behavior of birds. Three main operators and five species of birds (i.e. parthenogenetic, polyandrous, monogamous, polygynous, and promiscuous) are involved in the mating procedure. Two types of birds, including male and female exist in the society. Females are the most engaged genes in the society, while others are considered as males. The birds with the best fitness values among the society are selected to be parthenogenetic and polyandrous, and those with the worst values are assumed as promiscuous. The rest of the birds in the society are considered as monogamous and polygynous. Five mating systems are applied in the algorithm as follows [32].

i. In *Monogamy*, which is the most common system, a male bird mates with one female. The following shows the procedure of generating brood in this system:

$$X_b = X + \omega \times r. \times (X_i - X) \tag{21}$$

where X is a monogamous bird, and X_i is the female bird. X_b is the resultant brood.

ii. *Polygyny* refers to a mating system in which a male bird wants to mate with two or more females. In this procedure, only one brood whose genes are a combination of the females' genes is raised. The resulting brood is produced as follows:

$$X_b = X + \omega \times \sum_{j=1}^{n_i} r_j . \times (X_i - X) \tag{22}$$

iii. The mating system in which a chaotic mating event takes place is called *promiscuity*. In this system, breeding is the same as that of monogamous birds.

iv. In the *Parthenogenetic* system, each female changes her genes to improve its brood without mating with males.

v. In *polyandry*, a female bird, tending to mate with two or more males, chooses her desired males through a probabilistic method. This is while producing the brood is similar to the *polygyny* procedure.

The flowchart of the BMO algorithm is demonstrated in Fig. 7.

4.2.2. Multi-objective BMO (MOBMO)

In the bi-objective MG's economic/environmental dispatch, a multi-objective BMO (MOBMO) should be applied to optimize both total cost and emission, simultaneously. Therefore, a two-step sorting of initial population is applied. In the first step, the initial population is sorted according to the dominance concept. Hence, the most dominated solutions are eliminated in this step. Afterwards, in order to determine each group of female and male birds, if the remained solutions are more than one, they will be sorted based on the fuzzy clustering method [4]. Accordingly, the population is divided into five sections. The first two sections are assumed to be parthenogenetic and polyandrous birds, respectively, each constituting 5% of the society. The third section, which comprises 50% of the solutions, forms the monogamous. This is while the fourth section constitutes polygynous birds which is 30% of the society. The 10% remained solutions which are promiscuous birds are omitted in this step [32].

This procedure leads to an intelligent selection of female and male birds where the third and fourth sections of the society, which are the best males for mating, take part in the output Pareto front. Consequently, the actual Pareto optimal set is obtained in a shorter time.

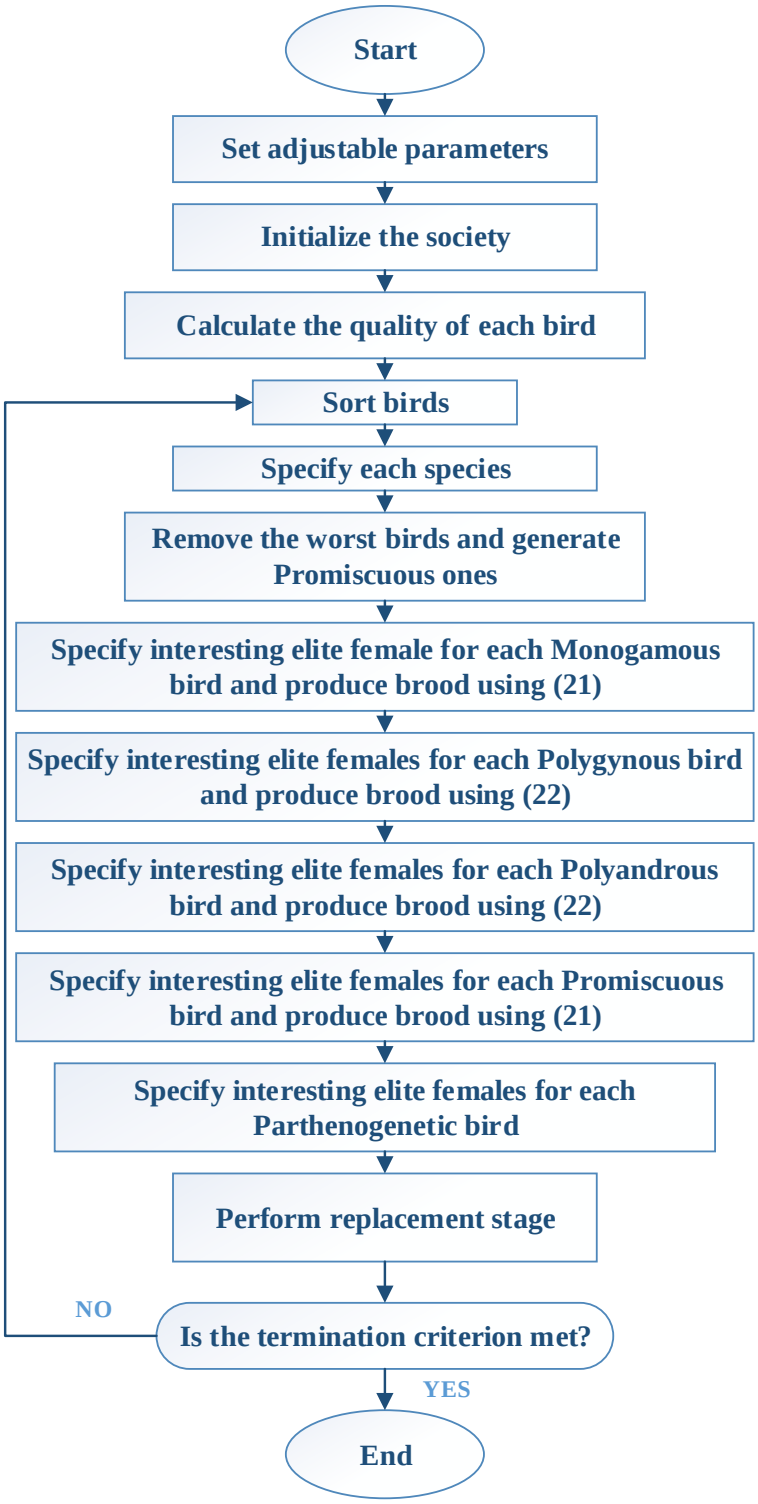

Fig. 7. Flowchart of BMO algorithm [32].

4.2.3. Modified Multi-objective BMO Algorithm (MMOBMO)

The improvement of the original BMO helps achieve a real Pareto optimal front in the MG's economic/environmental dispatch. Consequently, three modifications, one in the size of population and the other two in the mutations, are augmented to enhance the convergence ability and the accuracy of the approach.

The first modification: when the size of population is considered variable as in the following, the convergence speed of the algorithm increases:

$$N = round(\frac{(N_{\max} - N_{\min}) \times iteration}{iter_{\max}} + N_{\min}) \quad (23)$$

where N_{min} and N_{max} are the minimum and maximum populations, respectively, and $iter_{max}$ is the maximum number of iterations. An intelligent selection of the variable population size results in the increase of the population in each iteration; therefore, the population size is not fixed which helps to avoid getting trapped in local optima. As a result, the accuracy and speed of the algorithm will be improved.

The second modification: another modification to improve the accuracy of the proposed approach is carried out as follows:

Five constants $k_1 \neq k_2 \neq k_3 \neq k_4 \neq k_5$, all unequal to i, are chosen randomly from the population, while three constants $k_1' \neq k_2' \neq k_3'$ are selected randomly from the first, second and third sections of the repository, respectively. This leads to an intelligent search in the solution space. Four mutations are defined as:

$$mutation_1 = X_{k_1} + rand \times (X_{k_2} - X_{k_3}) \quad (24a)$$

$$mutation_2 = mutation_1 + rand \times (X_{best} - X_{worst}) \quad (24b)$$

$$mutation_3 = X_{k_4} + rand \times (X_{best} - X_{k_5}) \quad (24c)$$

$$mutation_4 = X_{k_1'} + rand \times (X_{k_2'} - X_{k_3'}) \quad (24d)$$

where after sorting the repository, the first non-dominated solution is selected as X_{best}, and in each iteration, the best non-dominated solutions are selected in turn as X_{best} such that all repository members take part in the population generation, while X_{worst} is the most dominated solution in the population.

The third modification: In order to increase the convergence speed of the algorithm, the third modification is augmented for each $X_{i,k}$ (i indicating each bird in the society, and k being the number of iteration). $X_{i,k}$ is an individual in the third and fourth sections of the population (i.e. the monogamous and polygynous birds which constitute 80% of the sorted population). Accordingly, one of the following is applied until the termination criterion is satisfied:

I. If $1 \leq k \leq \frac{1}{3} iter_{\max}$, select one of the mutations of (24) randomly and apply it to $X_{i,k}$ and X_{new1} is obtained. If $X_{i,k}$ does not dominate X_{new1}, X_{new1} will be saved in the repository, and $X_{i,k}$ is set equal to X_{new1}.

II. If $\frac{1}{3}iter_{\max}+1 \le k \le \frac{2}{3}iter_{\max}$, select two of the mutations of (24) randomly and apply them to $X_{i,k}$. X_{new1} and X_{new2} are achieved. Based on the non-dominance concept, determine the non-dominated solution among X_{new1}, X_{new2}, and then $X_{i,k}$ is determined and saved in the repository. In order to update $X_{i,k}$, one of the following is considered:

If both X_{new1} and X_{new2} are saved as non-dominated solutions, one of them is chosen based on (20), and $X_{i,k}$ is set to it.

If one of X_{new1} or X_{new2} is saved as the non-dominated solution, $X_{i,k}$ is set to it.

If none of X_{new1} and X_{new2} is saved as non-dominated solution, $X_{i,k}$ does not change.

III. If $\frac{2}{3}iter_{\max}+1 \le k \le iter_{\max}$, apply all four mutations of (24) and the non-dominated solutions among them, and $X_{i,k}$ are determined. Save the non-dominated solutions in the repository. The updating procedure of $X_{i,k}$ is done similar to the previous case (II).

If the number of saved non-dominated solutions among all mutations is more than one, choose one of them based on (20) and $X_{i,k}$ is set to it.

If one among all four mutations of (24) is saved as the non-dominated solution, then $X_{i,k}$ is set to it.

If none of the mutations of (24) is saved, $X_{i,k}$ maintains its previous value.

4.3. Application of the Proposed Methodology

In order to apply the proposed algorithm on the MG's optimal economic/emission dispatch, the following procedure shall be taken. First, the population size, number of design variables and the termination criterion is to be initialized. Problem information including MG properties and bids and power information of the DGs, storages and utility, hourly tidal and photovoltaic (PV) power forecasts and emission coefficients are then specified. The initial charge of the battery is also defined.

Since a mixed integer problem is considered in this paper, two types of variables, i.e. binary and continuous, are assumed. For states of generators as binary variables, u_i^t s are generated according to (6) as follows:

$$u_i^t = round(rand(.)\times(u_{i,\max}^t - u_{i,\min}^t) + u_{i,\min}^t) \qquad (25)$$

However, in order to consider the states of all units, u_i^t should satisfy the following condition for all hours:

$$\sum_{i=1}^{N_G} u_i^t.P_{Gi,\min}^t + P_{Grid,\min}^t \le P_{LD}^t \le \sum_{i=1}^{N_G} u_i^t.P_{Gi,\max}^t + P_{Grid,\max}^t \qquad (26)$$

If (26) is satisfied, a random population for continuous variables based on the achieved u_i^t s and according to (2) must be generated as:

$$P_{Gi}^t = rand(.)\times(P_{Gi,\max}^t - P_{Gi,\min}^t) + P_{Gi,\min}^t \quad (27a)$$

$$P_{si}^t = rand(.)\times(P_{si,\max}^t - P_{si,\min}^t) + P_{si,\min}^t \quad (27b)$$

$$P_{Grid} = rand(.)\times(P_{Grid,\max} - P_{Grid,\min}) + P_{Grid,\min} \quad (27c)$$

This is while the power constraints in (15)-(17) should also be satisfied. Since in the MG's optimal economic/environmental dispatch some limitations such as battery constraints depend on previous and future hours, X_{min} and X_{max} are functions of time. Accordingly, constraints change in different hours of the day [49]. Afterwards, the flowchart illustrated in Fig. 8. is applied for each particle to satisfy the power balance constraint. Additionally, the complete procedure and flowchart of the proposed MMOBMO algorithm is shown in Fig. 9.

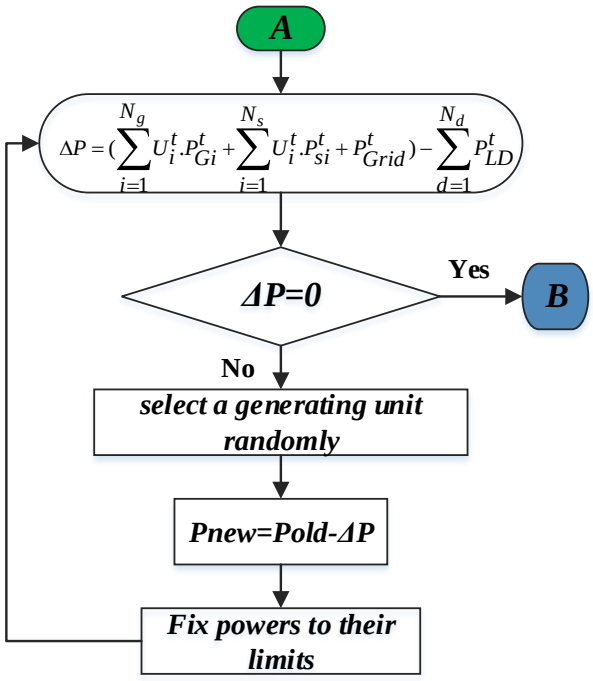

Fig. 8. Flowchart of power balance constraint.

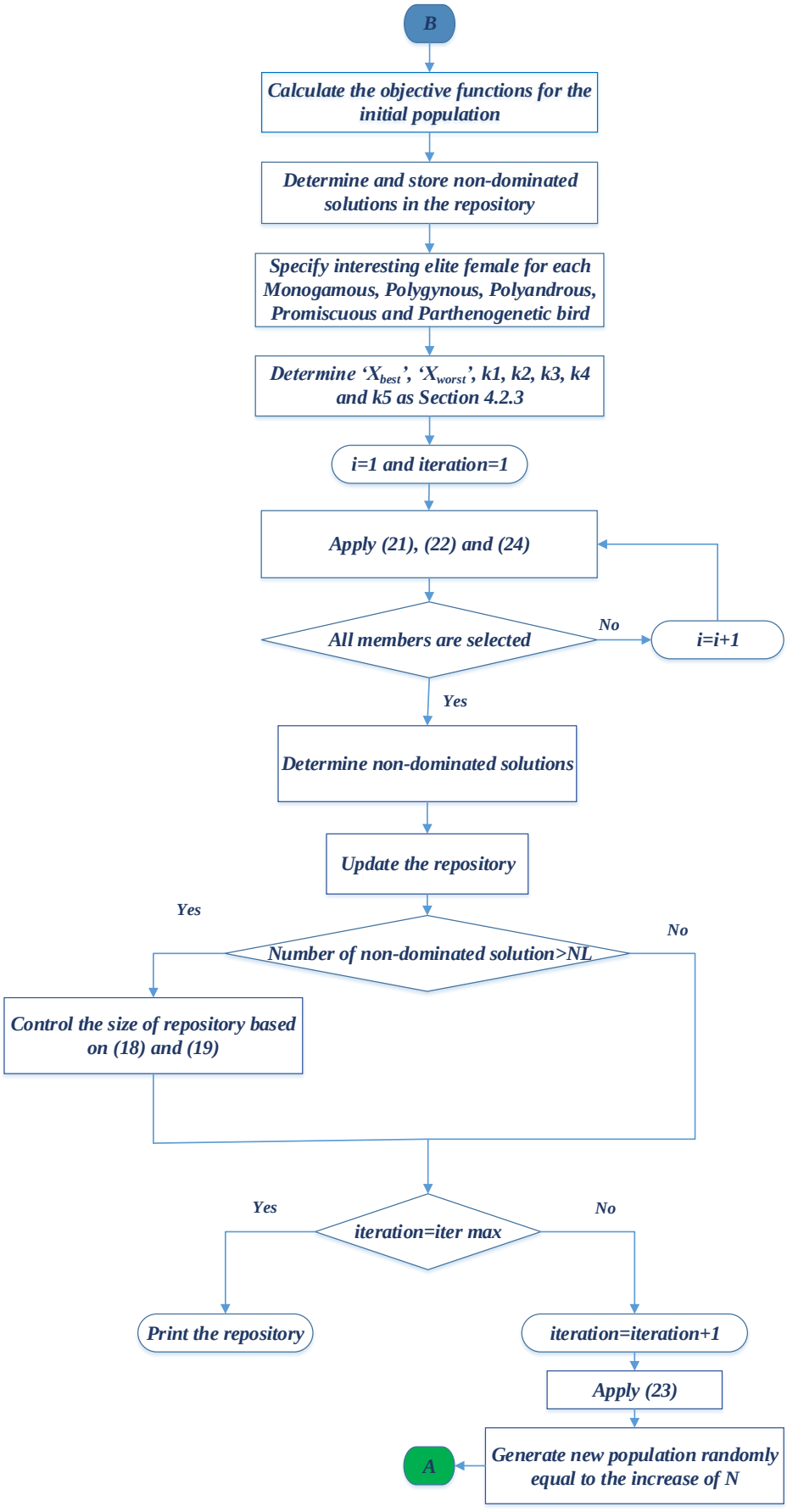

Fig. 9. Flowchart of the proposed MMOBMO algorithm.

5. Simulation Results

In order to verify the effectiveness and competitiveness of the proposed MMOBMO algorithm, two cases are inspected in this section. In Case I, the proposed MMOBMO is first compared with the algorithms of [50] through applying on three test functions. Results are reported from 40 independent runs of each algorithm. Afterwards, in Case II, to survey the efficiency of MMOBMO algorithm in solving economic\environmental dispatch of an MG in the presence of tidal turbine, the data of SLMG are used in order to investigate the considered problem [33]. In this case, first in the cost objective function of (8) the battery degradation cost is ignored and results are discussed in two different scenarios. Finally, simulation results for the case in which the battery degradation cost is taken into account are revealed.

Case I: In this part, three different test functions are chosen from [50], and the proposed MMOBMO algorithm is applied to solve the problems.

-Test Function 1: The first example taken from [50] is as follows:

$$\begin{aligned} &Minimize \quad f_1(\vec{x}) = \sum_{i=1}^{n-1}(-10\exp(-0.2\sqrt{x_i^2 + x_{i+1}^2})) \\ &Minimize \quad f_2(\vec{x}) = \sum_{i=1}^{n}(|x_i|^{0.8} + 5\sin(x_i)^3) \end{aligned} \tag{28}$$

where $-5 \le x_1, x_2, x_3 \le 5$

In Fig. 10. a comparison between the Pareto front of the proposed MMOBMO and those of [50] is illustrated and the better performance of the proposed algorithm in solving the first chosen test function is observed.

-Test Function 2: The second test functions are proposed in [50] as:

$$\begin{aligned} &Minimize \quad f_1(x_1, x_2) = x_1 \\ &Minimize \quad f_2(x_1, x_2) = g(x_1, x_2).h(x_1, x_2) \end{aligned} \tag{29}$$

where

$$\begin{aligned} &g(x_1, x_2) = 11 + x_2^2 - 10.\cos(2\pi x_2) \\ &h(x_1, x_2) = \begin{cases} 1 - \sqrt{\dfrac{f_1(x_1, x_2)}{g(x_1, x_2)}}, & if \quad f_1(x_1, x_2) = x_1 \\ 0, & otherwise \end{cases} \end{aligned} \tag{30}$$

and $0 \le x_1 \le 1, \quad -30 \le x_2 \le 30$

In Fig. 11. a comparison between the Pareto front of the proposed MMOBMO and those of [50] is illustrated and the better performance of the proposed algorithm in solving the second chosen test function is shown.

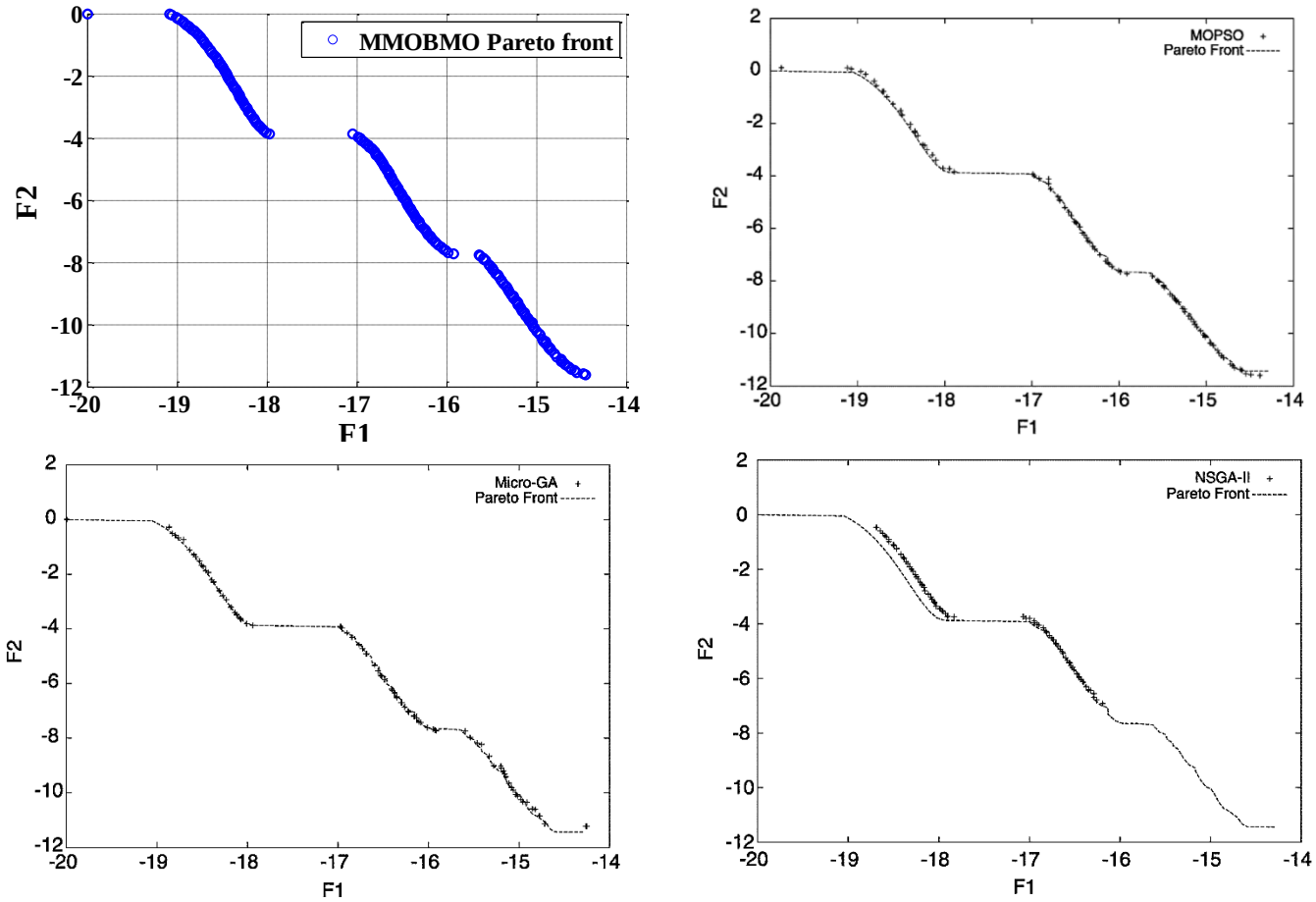

Fig. 10. Comparison between the Pareto front of the proposed MMOBMO and results of [50] for Test Function 1.

-Test Function 3: The third test function is [50]:

$$\begin{aligned} &\textit{Minimize} \quad f_1(x_1, x_2) = x_1 \\ &\textit{Minimize} \quad f_2(x_1, x_2) = \frac{g(x_2)}{x_1} \end{aligned} \tag{31}$$

$$g(x_2) = 2 - \exp\left\{-\left(\frac{x_2 - 0.2}{0.004}\right)^2\right\} - 0.8\exp\left\{-\left(\frac{x_2 - 0.6}{0.4}\right)^2\right\} \tag{32}$$

and $0.1 \le x_1 \le 1, \quad 0.1 \le x_2 \le 1$

A comparison between the Pareto front of the proposed MMOBMO and results of [50] is shown in Fig. 12. The better performance of the proposed algorithm compared with other algorithms in solving the third test function is proved.

From the comparison made in this section, the effective performance of the proposed MMOBMO in solving multi-objective problems can be concluded.

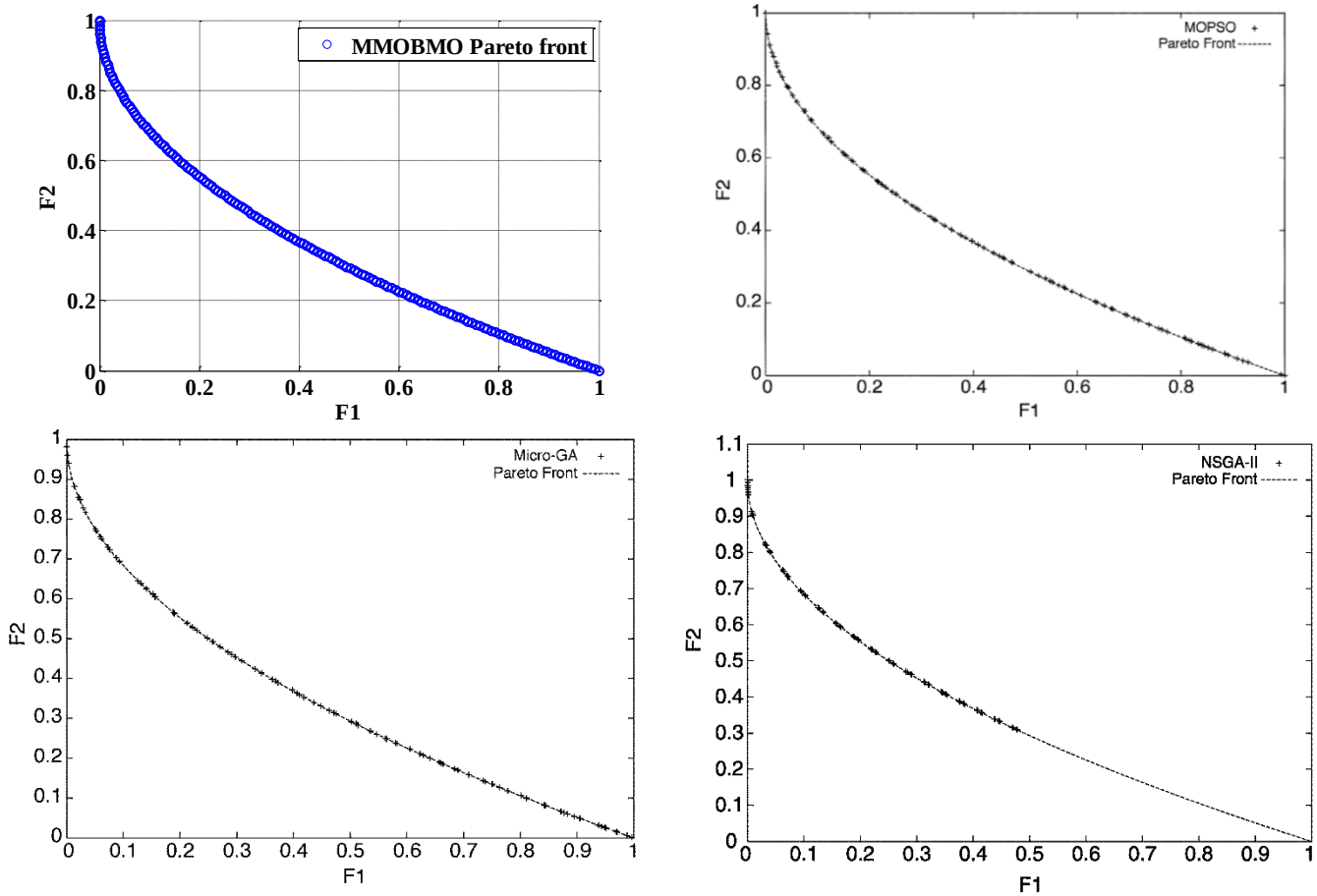

Fig. 11. Comparison between the Pareto front of the proposed MMOBMO and results of [50] for Test Function 2.

Case II: The efficiency of the proposed MMOBMO algorithm in solving the economic\emission dispatch of an MG in the presence of tidal turbine is contemplated. This is while the data of SLMG are used in order to investigate the considered problem [33]. The MG of Fig 1. is considered as the test system. For the sake of clarity of the performance of each power unit, a 24 h scheduling scheme is assumed for the analysis of the simulated system. Besides, the unity power factor is considered for all DGs; thus, they just produce active power. In order to exploit the market more profitably, power exchange between the MG and the utility is allowed at any hour during the day. Decision about this power exchange is done by the MG central controller (MGCC) [4]. The data for the hourly active power of PV and tidal turbine are shown in Fig 13. The utility power production bids and forecasted load demand on the specifically chosen day August 5, 2016 are available in figures 14 and 15, respectively. In Table 1 the entire bid data for all DGs along with the utility grid are available. The amount of emission of DGs is also available in Table 1. All loads are electrical and no thermal load is considered. Since PV and tidal units do not consume any fuel at the times when they produce electrical power during the day, the utility has to buy all electrical power produced by these units. As mentioned in previous sections, two incompatible objectives (i.e. cost and emission) are dealt with in this paper. Therefore, a Pareto-optimal set is attained for the problem. It is assumed that PV and tidal are in service all through the day and are accepted to exploit at their maximum available output powers. This is while the ON\OFF states of the dispatchable DGs (i.e. FC and MT) are considered. Therefore, in the algorithm process, solutions for dispatchable units are compared with their minimum limit powers and in case lower, the power will be put to zero. To the best of our knowledge, this case has not been considered in the literature.

The proposed method was implemented in MATLAB 8.1 and solved with a laptop computer with Core i5 CPU and 4GB ~~of~~ RAM. The population and number of maximum iterations are both considered 100.

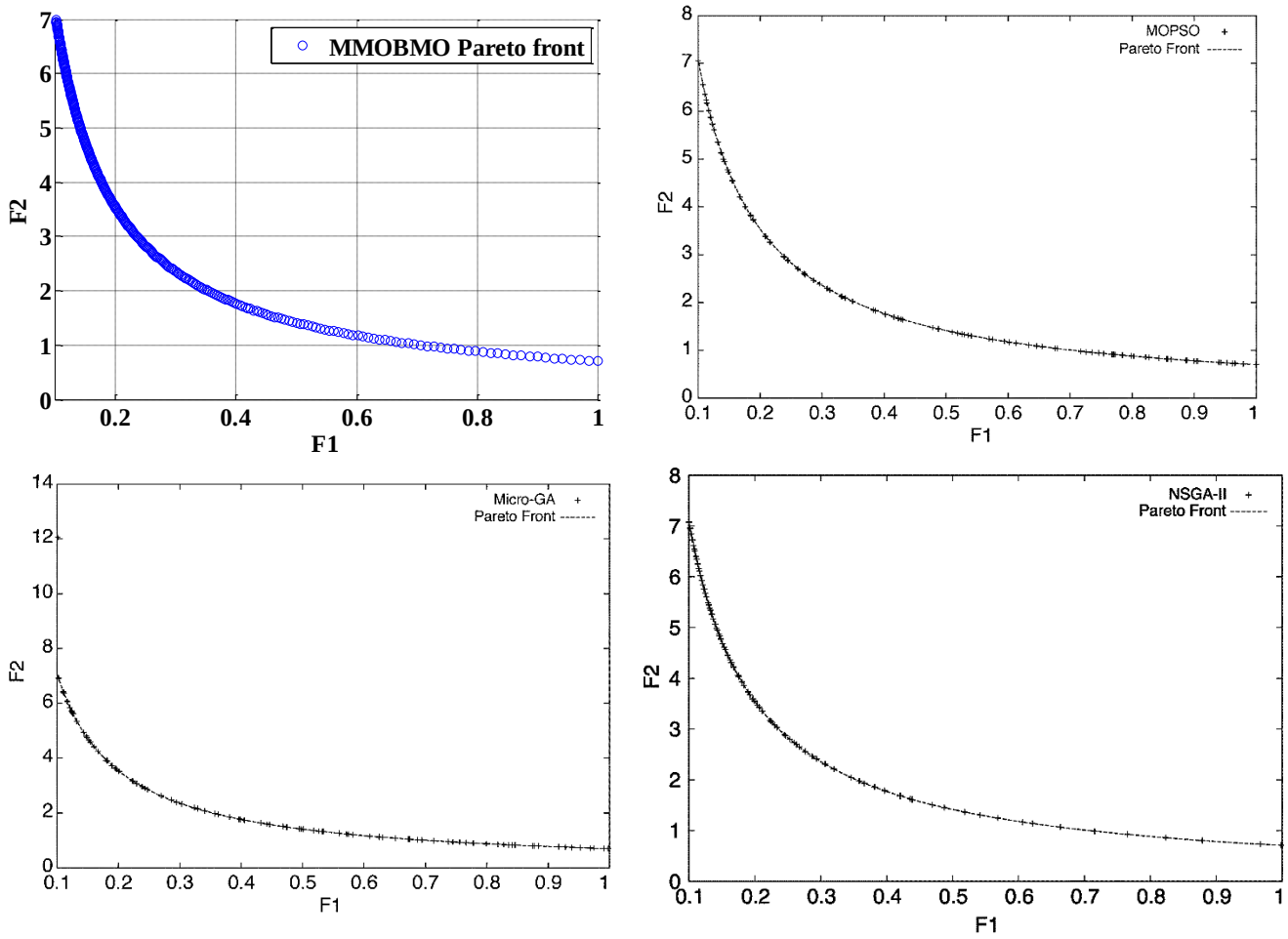

Fig. 12. Comparison between the Pareto front of the proposed MMOBMO and results of [50] for Test Function 3.

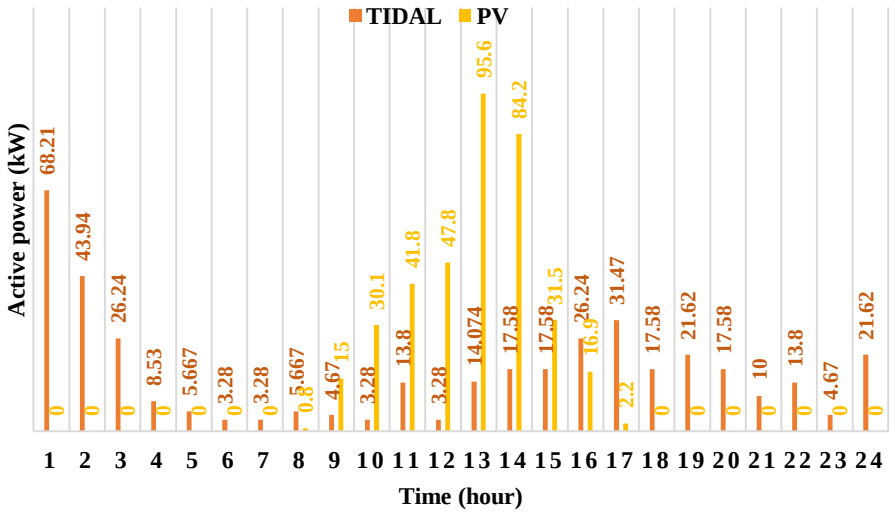

Fig. 13. The hourly active power of PV and tidal turbine [33].

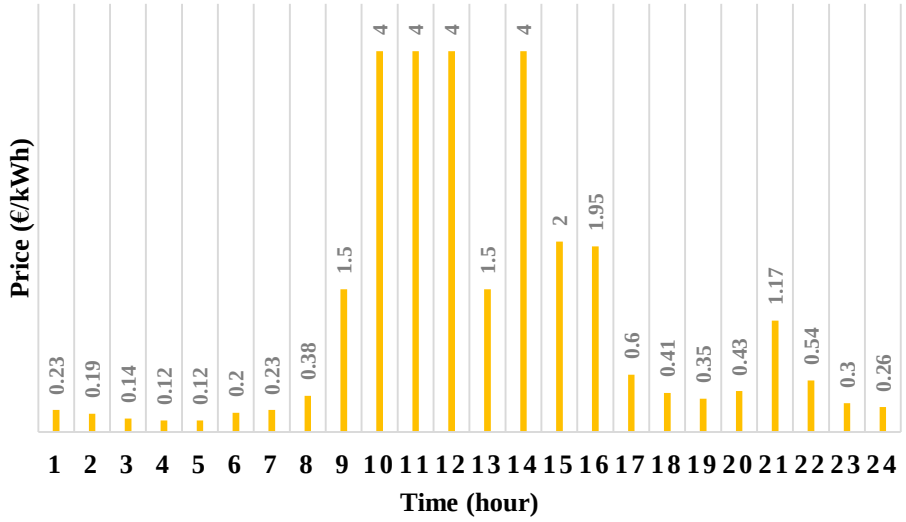

Fig. 14. The hourly market price.

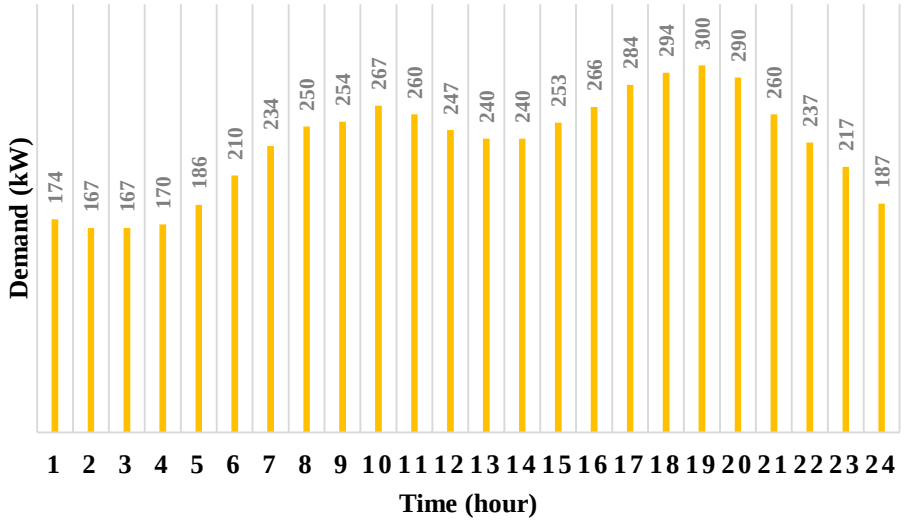

Fig. 15. The hourly load demand [33].

Table 1. Bids and emissions of DG sources and the power market [4].

Type	Bid(€/kWh)	Startup/shut down cost (€)	CO_2(kg/kWh)	SO_2(kg/kWh)	NO_x(kg/kWh)
MT	0.475	2.88	0.72	0.0036	0.1
FC	0.294	4.95	0.46	0.003	0.007
PV	2.584	0	0	0	0
TST	0.4	0	0	0	0
Batt	0.38	0	0.01	0.0002	0.0001
Market	-	-	0.9215	0.0036	0.0023

5.1. First Scenario

In this section, it is supposed that all dispatchable DGs in the MG are in service. TST and PV are assumed to exploit at their maximum available output powers. Two sub-scenarios are then considered. In the first, no limits are put on the battery initial charge, while in the second the initial charge is expected to be zero; hence, in the latter case in order to be able to discharge at later hours, the battery should first be charged.

The Pareto optimal fronts of the two sub-scenarios are revealed in figures 16 and 17, and results for three algorithms, including the original BMO, PSO and the proposed MMOBMO, are compared, and the best compromised solutions for both cases are depicted. It is obvious that when MMOBMO is applied, the Pareto optimal front maintains between the points where the two objective functions are in their minimum values. When the cost function is in its minimum value, i.e. 908.4 €, emission is 2740 kg. In this case, when cost is considered as the only objective function, the global best solution is achieved. Besides, when emission is decreased to 1396 kg, the cost will equal 2869 €. The best compromised solution is calculated according to the procedure described in Section 6 where the cost and emission objective functions are 1206 € and 1794kg, respectively.

Fig. 17. demonstrates the Pareto optimal front for the second sub-scenario and solutions for three algorithms, namely the original BMO, PSO and MMOBMO, are compared. When employing MMOBMO, the Pareto front remains between the point where cost and emission are in their minimum values. When the cost function is in its minimum value, i.e. 1252 €, the emission objective function equals 3739 kg whereas in the point where emission is reduced to 2926 kg the cost function equals 3094 €. In this case, the best compromised solution is when the cost and the emission objective functions are 1797 € and 3271 kg, respectively.

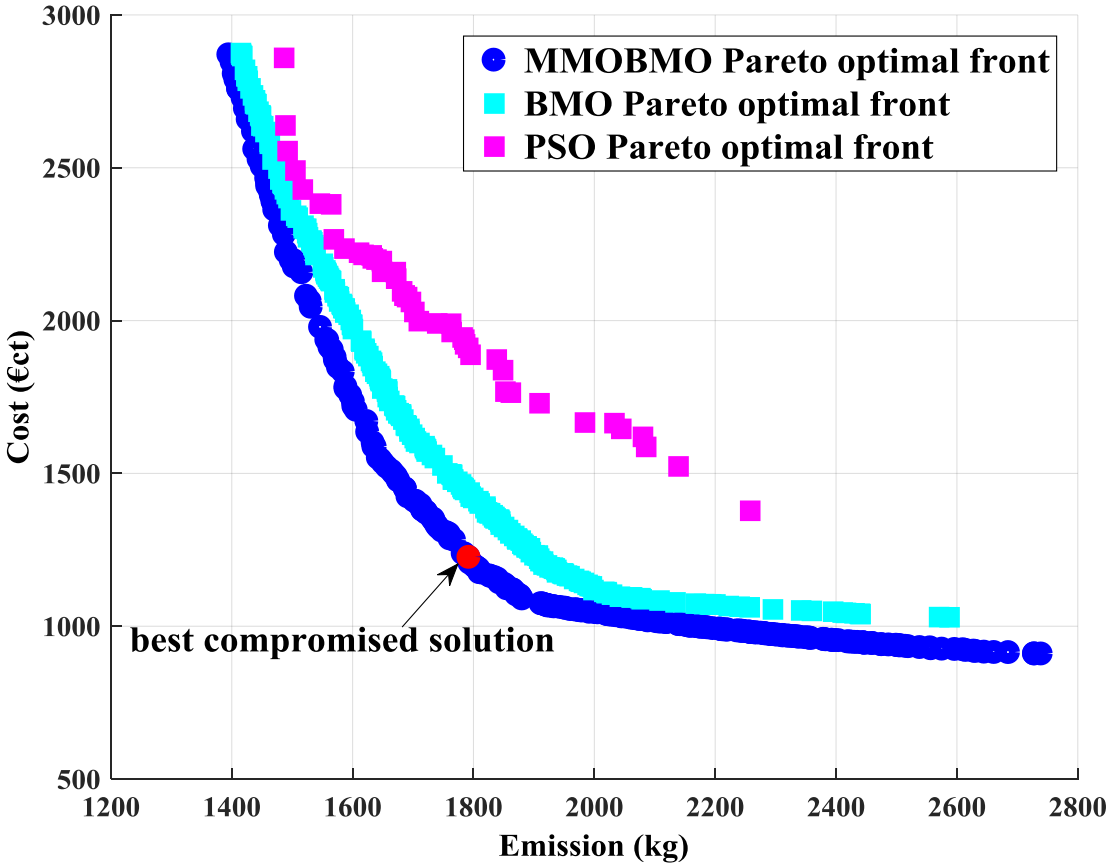

Fig. 16. Pareto optimal fronts of MMOBMO, BMO and PSO: first sub-scenario (first scenario).

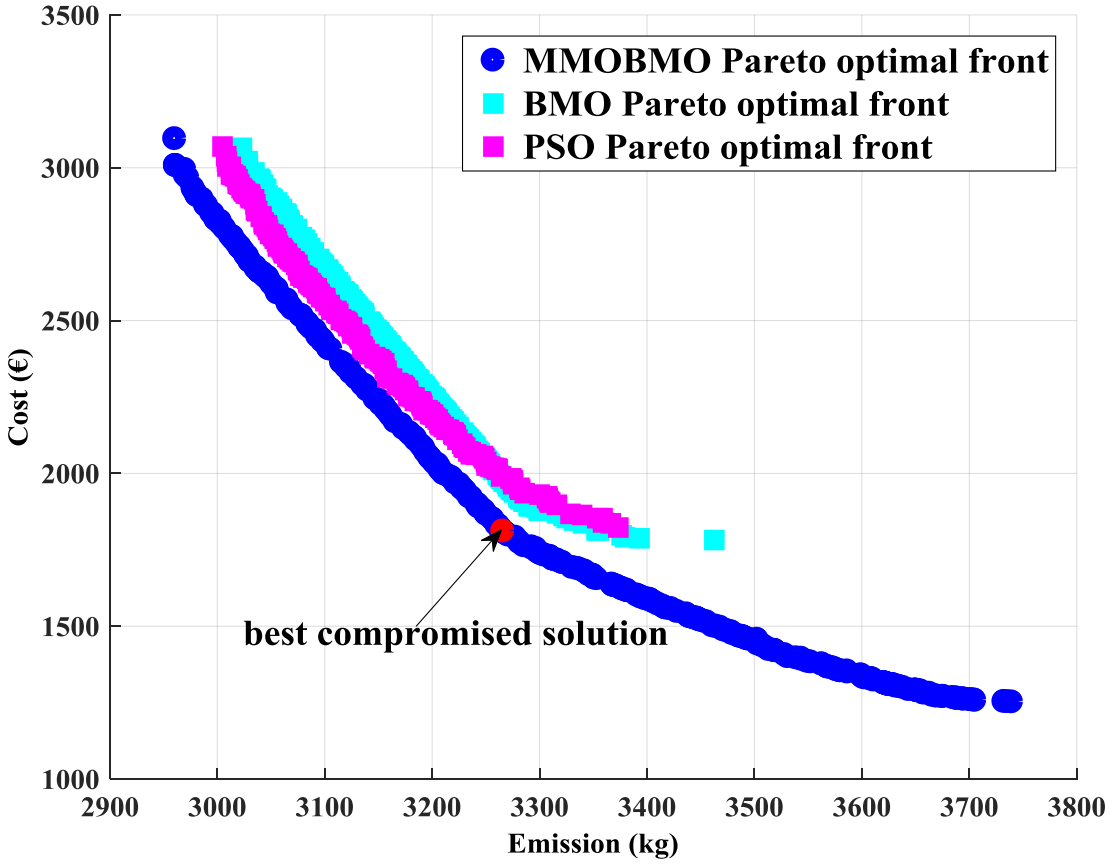

Fig. 17. Pareto optimal fronts of MMOBMO, BMO and PSO: second sub-scenario (first scenario).

5.2. Second Scenario

The difference between this scenario and the first scenario is that the ON\OFF states of dispatchable DGs (i.e. FC and MT) are herein considered. Therefore, in the algorithm process, the solutions for dispatchable units are compared with their minimum powers' limits and if lower, the power will be put to zero.

The second scenario is divided into two sub-scenarios as was the first scenario (in the first sub-scenario the battery initial charge is unlimited while in the second the initial charge is expected to be zero). The Pareto optimal solutions for the first sub-scenario are illustrated in Fig. 18, where the best compromised solution for the proposed MMOBMO is revealed. Besides, a comparison between the three algorithms, BMO, PSO and MMOBMO, is performed. The Pareto optimal front is kept between the points where the two objective functions are in their minimum values. It is evident that where the cost function is in its minimum value, 898.9 €, emission is 2792 kg; besides, when emission is decreased to 1390 kg, cost equals 2874 €. The best compromised solution is where the cost and emission objective functions are 1124 € and 1839 kg, respectively.

Fig. 19. demonstrates the Pareto optimal front for the second sub-scenario. Results for the original BMO, PSO and MMOBMO are compared. Obviously, the Pareto front for MMOBMO maintains between the point where cost

and emission are in their minimum values. When the cost objective function is in its minimum value, i.e. 1283 €, emission equals 3694 kg; however, when emission is reduced to 2929 kg, the cost objective function equals 3126 €. In this case, the best compromised solution is when the cost and emission objective functions are 1805 € and 3264 kg, respectively.

In both of the second sub-scenarios, where the initial charge of the battery is zero, a strict restriction on the battery charge and discharge is put on. Consequently, the most adjustable scenario is when the battery has initial charge.

As mentioned, in multi-objective problems, the superiority of an optimization algorithm can be concluded from its appropriate and fast convergence while attaining a well-distributed Pareto front. According to the results, it is proved that the proposed MMOBMO has successfully fulfilled these assumed criteria, and it can significantly achieve the exceptional solution in comparison with other methods in solving multi-objective optimal operation management of an MG.

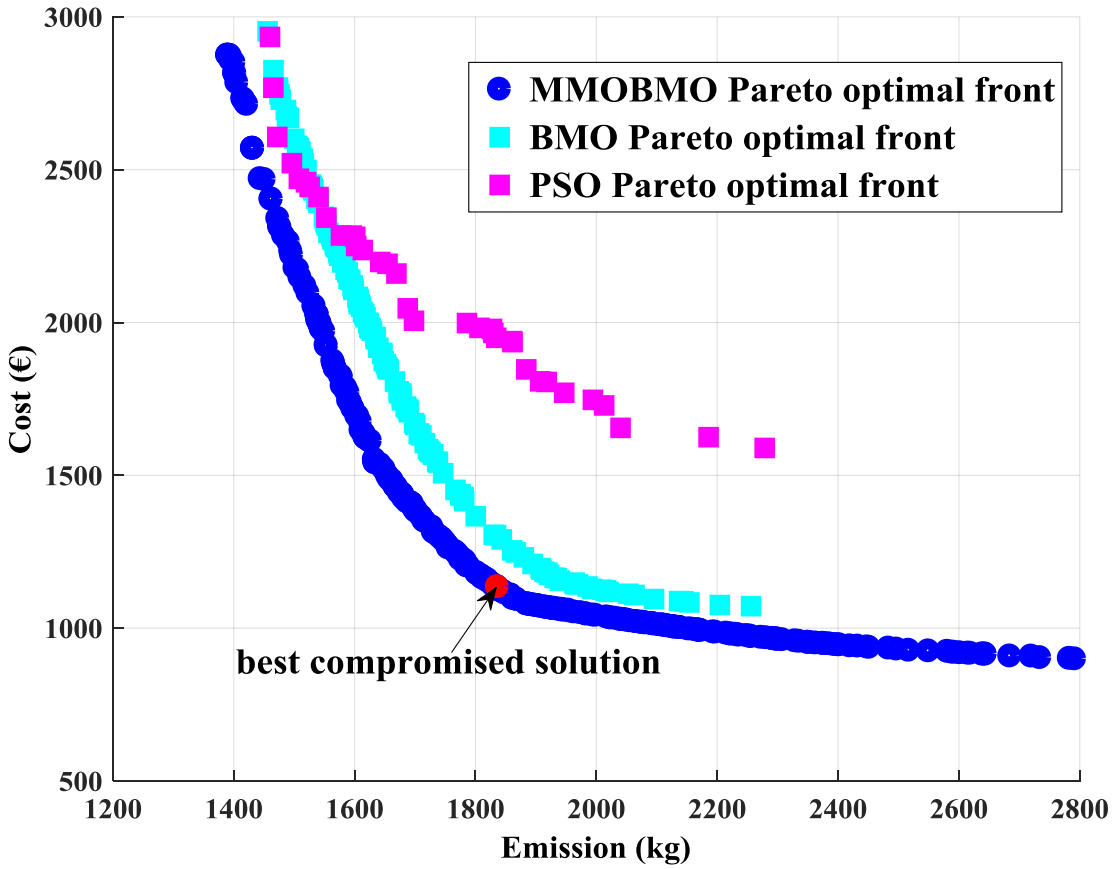

Fig. 18. Pareto optimal fronts of MMOBMO, BMO and PSO: first sub-scenario (second scenario).

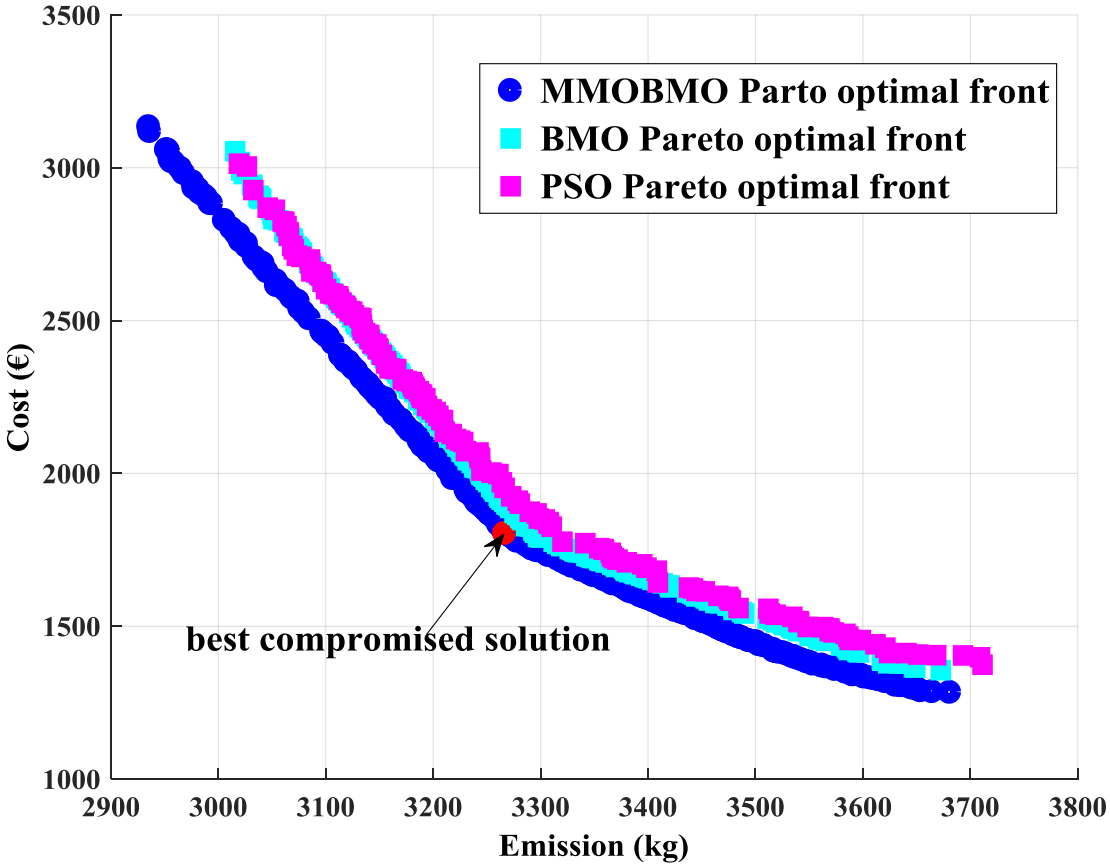

Fig. 19. Pareto optimal fronts of MMOBMO, BMO and PSO algorithms: second sub-scenario (second scenario).

In order to scrutinize the detailed model of the storage device in the considered MG energy management problem, the battery degradation cost is added to (8) and results are illustrated in Fig. 20. Moreover, the battery SOC_{min} and SOC_{max} are respectively fixed as 10% and 90% of the total battery capacity. Additionally, the initial SOC of the battery equals to SOC_{min} which results in the best performance and minimum total operation costs. Furthermore, the final SOC value should equal to the starting SOC in order to have the system optimal dispatching [26]. The parameters of the Li-ion battery are tabulated in Table 2 in details. The same conditions as the second sub-scenario of the first scenario is considered in this case in order to compare the results.

Table 2. Parameters of Li-ion battery.

Lithium-ion battery	
Total energy storage, kWh	300
Efficiency	≥ 93%
Cost of battery, €/kWh	247

Fig. 20. demonstrates the Pareto optimal front of the proposed MMOBMO for the case in which the battery degradation cost is considered in the problem. When the cost function is in its minimum value, i.e. 1938 €, the emission objective function equals 3494 kg, while in the point where emission is reduced to 2975 kg, the cost function equals 3206 €.

Tables 3 and 4 reveal the hourly power dispatch of the points where, respectively, cost and emission objective functions are minimum. Accordingly, it is evident that all equality and inequality constraints are satisfied. In the columns related to the dispatch of the battery, the negative values are representative of the times where the battery is charging while the positive values are related to the times where the battery is in the discharging mode. However, in the columns related to the dispatch of the utility, the negative values are representative of delivering energy to the upstream network, while the positive values are related to the times when energy is purchased from the upstream network.

Energy storage devices can improve the MGs operation from economic, resiliency and reliability points of view. The strategy of using storage devices in MGs is to store energy when the load level is low while delivering the stored energy in peak hours.

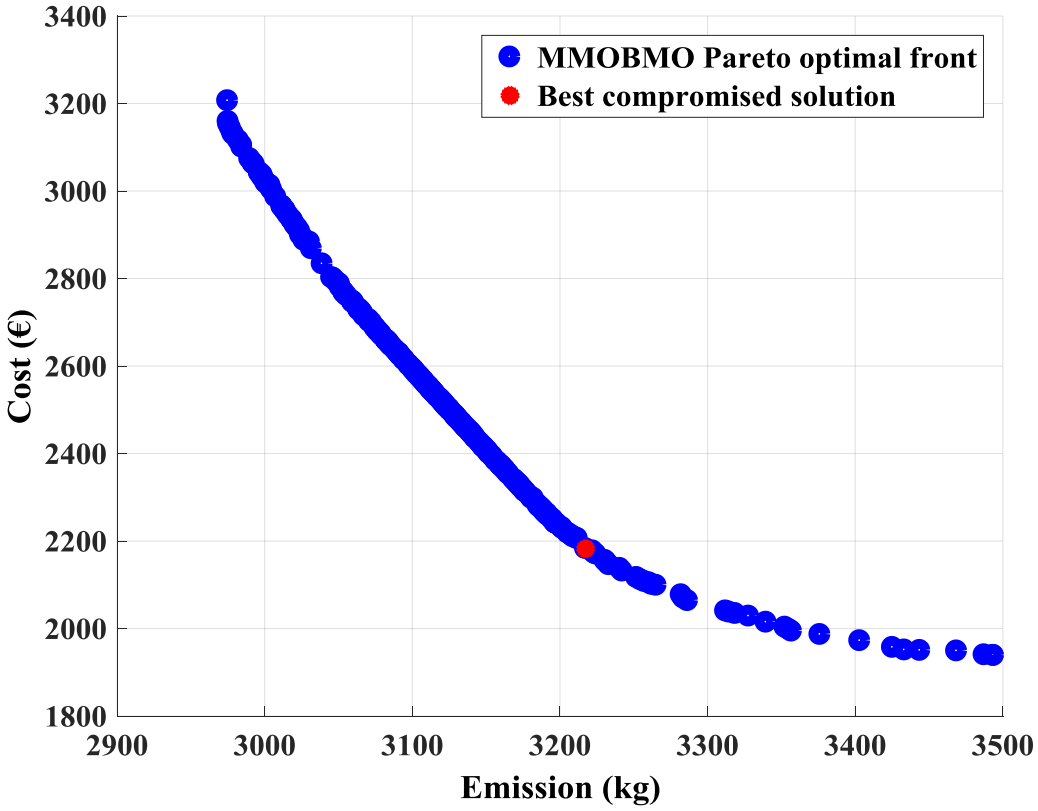

Fig. 20. Pareto solutions of the proposed MMOBMO algorithm while considering the battery degradation cost.

As is observed from Table 3 and figures 14 and 15, in the first 8 hours of the planning horizon where the market price is low, the system operator purchases the demanded energy from the utility. This energy can either be utilized to satisfy the demand or be stored in the storage device. The stored energy will then be sold to the upstream network in peak hours with a higher price. Using this strategy, the system operator can provide an economical MG scheduling.

According to Table 3, since the initial energy of the battery is considered to be equal to $SOC_{\min}$, the system operator purchases power from the upstream network. This power along with the generating power of DG units are used to satisfy the local load while the excess energy is stored in the battery. This will continue until the energy of the battery reaches $SOC_{\max}$ which occurs at the end of hour 3. Afterwards, up to hour 10 the battery is not charged nor discharged. At hour 10, the load increases and the corresponding price reaches to its maximum value. Consequently, the best strategy is that the battery starts discharging and the stored energy along with DGs' generated powers are sold to the upstream network. This strategy continues up to hour 12 until when the SOC of the battery equals $SOC_{\min}$. At hour 13 since the market price is low energy is purchased from the upstream network and this stored energy is sold to the utility at the next hour as the market price is at maximum value at hour 14. Then, at hour 14 the battery is completely discharged. From hour 15 to hour 24, during which the market price is approximately low, the power is purchased from the upstream network and the battery is not charged nor discharged. It is concluded from the results that the proposed MMOBMO algorithm can follow a proper strategy in order to use the storage device and the power exchange link with the upstream network in order to minimize the MG total operational cost.

Table 3. The best solution for minimizing the cost objective function.

Hour	MT	FC	TST	PV	Battery	Utility	Load
1	20	85.79	68.21	0	-100	100	174
2	23.06	100	43.94	0	-100	100	167
3	20	73.39	26.24	0	-52.63	100	167
4	20	41.47	8.53	0	0	100	170
5	20	60.33	5.67	0	0	100	186
6	20	86.72	3.28	0	0	100	210
7	30.72	100	3.28	0	0	100	234
8	43.53	100	5.67	0.80	0	100	250
9	100	100	4.67	15	0	34.33	254
10	100	100	3.28	30.1	100	-66.38	267
11	100	100	13.8	41.8	100	-95.6	260
12	100	100	3.28	47.8	28	-32.08	247
13	100	100	14.07	95.6	-42.35	-27.33	240
14	100	100	17.58	84.2	38.20	-99.99	240
15	100	100	17.58	31.5	0	3.92	253
16	100	100	26.24	16.9	0	22.86	266
17	100	100	31.47	2.2	0	50.33	284
18	76.42	100	17.58	0	0	100	294
19	78.39	100	21.62	0	0.00	100	300
20	91.88	100	17.58	0	0.00	80.54	290
21	100	100	10	0	0	50	260
22	100	100	13.8	0	0	23.2	237

23	20	100	4.67	0	0	92.33	217
24	20	45.38	21.62	0	0	100	187

According to tables 1 and 4, since the emission coefficient of the upstream network is considerably high, in order to minimize the pollutant emission the demand is satisfied from MG resources except for the hours where the demand is more than the total generated power of the MG. Consequently, the MT and FC produce their maximum powers during all hours of the day. The battery charging and discharging patterns are different from the previous case (i.e. when the cost objective function is in its minimum value). When the total generated powers of MT, FC, TST and PV are more than the demanded load, the excess energy is stored in the battery which is occurred in the first 5 hours of the day according to Table 4. From hour 6 to 11, during which the demanded load increases, the battery is discharged in order to satisfy the load. From hour 12 to 14, since the load demand decreases, the battery recharges. From hour 15 to 19 the battery discharges to prevent using the upstream network energy such that the emission minimizes. At hour 19 the battery is completely discharged and the SOC of the battery equals $SOC_{\min}$ and in order to satisfy the rest of the demand the power is purchased from the upstream network. At hour 20 to 23 in order to satisfy the load the MG operator needs to purchase energy from the upstream network. At hour 24, as the demanded load is less than the total MG's power produced, there is no need to additional power. Furthermore, since the emission coefficient of FC is less than MT, the FC continues to produce power at its maximum value and the MT's produced power equals the difference of the demanded load and the total power produced by FC and TST.

Table 4. The best solution for minimizing the emission objective function.

Hour	MT	FC	TST	PV	Battery	Utility	Load
1	100	100	68.21	0	-94.21	0	174
2	64.04	100	43.94	0	-40.98	0	167
3	100	100	26.24	0	-59.24	0	167
4	100	100	8.53	0	-38.53	0	170
5	100	100	5.67	0	-19.67	0	186
6	100	100	3.28	0	6.72	0	210
7	100	100	3.28	0	30.72	0	234
8	100	100	5.67	0.80	43.53	0	250
9	100	100	4.67	15	34.33	0	254
10	100	100	3.28	30.1	33.62	0	267
11	100	100	13.8	41.8	4.4	0	260
12	100	100	3.28	47.8	-4.08	0	247
13	100	100	14.07	95.6	-69.67	0	240
14	100	100	17.58	84.2	-61.78	0	240
15	100	100	17.58	31.5	3.92	0	253
16	100	100	26.24	16.9	22.86	0	266
17	100	100	31.47	2.2	50.33	0	284
18	100	100	17.58	0	76.42	0	294
19	100	100	21.62	0	43.46	34.92	300
20	100	100	17.58	0	0	72.42	290
21	100	100	10	0	0	50	260
22	100	100	13.8	0	0	23.2	237
23	100	100	4.67	0	0	12.33	217
24	65.38	100	21.62	0	0	0	187

According to Fig. 20. in the point where the cost objective function is in its minimum value, the emission is in its maximum value and vice-versa. Therefore, the two considered objective functions conflict each other. Using the achieved optimal Pareto front of Fig. 20. and the best compromised solution concept according to (20), a trade-off solution among the results of both objective functions is presented for the multi-objective MG energy management. In this case, the best compromised solution is when the cost and the emission objective functions are 2183 € and 3217 kg, respectively as is shown in Fig. 20. The hourly power generation of each dispatchable units along with the battery's charge/ discharge and the utility import/export of the best compromised solution in this case are presented in Table 5.

In order to show the real application of the proposed MMOBMO algorithm in short-term MG scheduling, another test system is considered in which the number of DG units is increased. In other words, the second test MG consists of five FC and MT units, four batteries, three TSTs and eight PV units. Moreover, the maximum exchangeable power and the demanded load increase five times. The resulted Pareto optimal front of this case is illustrated in Fig. 21. In this case, the best compromised solution is when the cost and the emission objective functions are 9638 € and 17620 kg, respectively.

Table 5. Best compromised solution for the case where battery degradation cost is taken into account.

Hour	MT	FC	TST	PV	Battery	Utility	Load
1	99.70	100	68.21	0	-94.93	1.02	174
2	100	100	43.94	0	-76.94	0	167
3	92.02	99.91	26.24	0	-52.09	0.92	167
4	86.57	99.96	8.53	0	-25.06	0	170
5	83.09	100	5.67	0	-2.76	0	186
6	99.74	100	3.28	0	0	6.98	210
7	100	100	3.28	0	0	30.72	234
8	99.89	100	5.67	0.80	0	43.64	250
9	100	99.84	4.67	15	18.2	16.29	254
10	100	100	3.28	30.1	64.96	-31.34	267
11	100	100	13.8	41.8	95.18	-90.78	260
12	100	100	3.28	47.8	49.43	-53.81	247
13	100	99.91	14.07	95.6	-69.58	0	240
14	99.95	99.92	17.58	84.2	38.35	-100	240
15	100	99.77	17.58	31.5	4.15	0	253
16	100	100	26.24	16.9	19.75	3.11	266
17	100	100	31.47	2.2	0	50.33	284
18	100	100	17.58	0	0	76.42	294
19	99.77	99.96	21.62	0	0	78.65	300
20	100	100	17.58	0	0	72.42	290
21	100	100	10	0	0	50	260
22	100	100	13.8	0	0	23.2	237
23	100	100	4.67	0	0	12.33	217
24	63.31	100	21.62	0	0	2.07	187

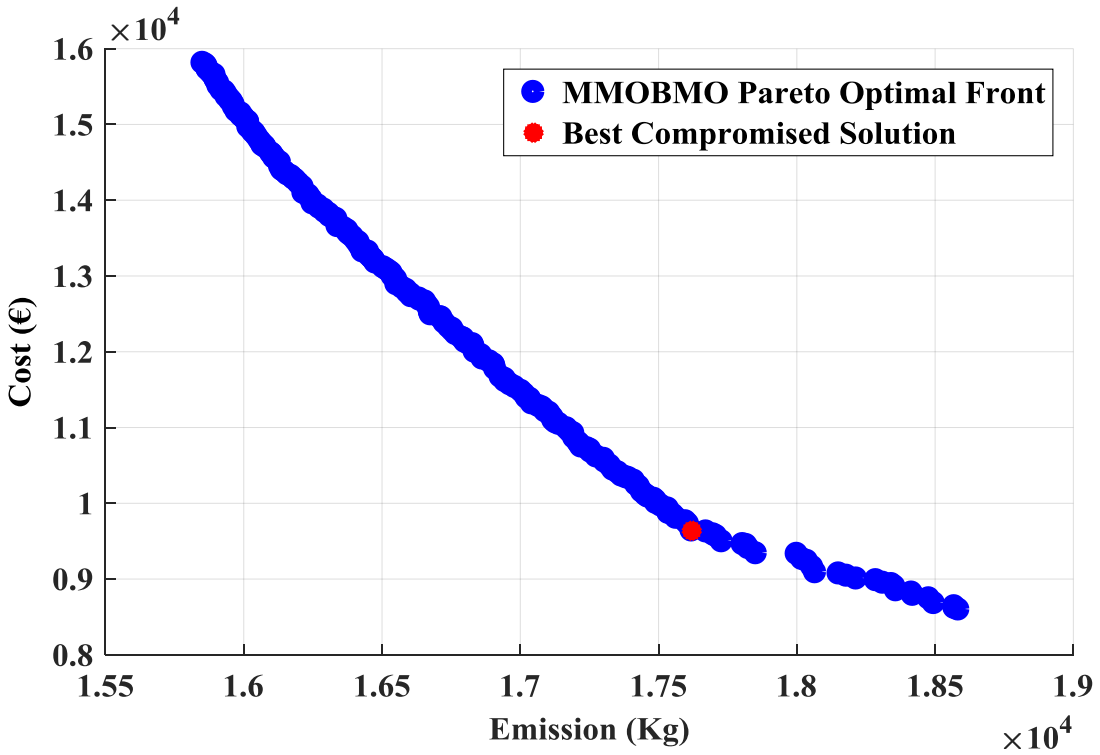

Fig. 21. Pareto solutions of the proposed MMOBMO algorithm for the second test MG.

6. Conclusions

The effects of implementing the practical tidal stream turbine (TST) of Lake Saroma green microgrid (SLMG) in a typical MG were dealt with in this paper. The optimal energy management of the system was investigated using the proposed MMOBMO algorithm, while a new economic/environmental model for the practical TST along with a detailed economic model for storage devices were presented. It was observed that since PV and tidal generators are complementary, an MG consisting of these two generators is more proper in sustainably supplying load. In order to demonstrate the effective performance of the proposed algorithm, two different cases were studied. Moreover, the ON/OFF states of dispatchable DGs were taken into account. Consequently, the superiority of the algorithm in dealing with mixed-integer problems in comparison with PSO and the original BMO was verified. In addition to economic advantages, since tidal energy is well predictable, it was suggested that in regions with high potential of harnessing tidal energies, other renewable units shall be replaced by tidal generators. Future works can include the following:

i) Considering the uncertainties of renewable resources including tidal and PV generators and solving the probabilistic MG's energy management.

ii) Investigating demand response and electric vehicles' effects along with other elements of the future smart grid in the considered MG's energy management.

iii) Inspecting reliability subject as an objective function in the MG's optimal operation.

Acknowledgement

Appreciation is offered to the Iran National Science Foundation for a grant to collect data for this research. The authors wish to thank the Iran National Science Foundation for supporting helps to do this research and providing this opportunity for the survey team. Also, this work was supported in part by Royal Academy of Engineering Distinguished Visiting Fellowship under Grant DVF1617\6\45.

References

1. A. Kavousi-Fard, "A Hybrid Accurate Model for Tidal Current Prediction," *IEEE Transactions on Geoscience and Remote Sensing,* vol. 55, pp. 112-118, 2016.
2. A. Kavousi-Fard, "A Novel Probabilistic Method to Model the Uncertainty of Tidal Prediction," *IEEE Transactions on Geoscience and Remote Sensing,* vol. 55, pp. 828-833, 2017.
3. R. H. Zubo, G. Mokryani, H.-S. Rajamani, J. Aghaei, T. Niknam, and P. Pillai, "Operation and planning of distribution networks with integration of renewable distributed generators considering uncertainties: A review," *Renewable and Sustainable Energy Reviews,* 2016.
4. A. A. Moghaddam, A. Seifi, T. Niknam, and M. R. A. Pahlavani, "Multi-objective operation management of a renewable MG (micro-grid) with back-up micro-turbine/fuel cell/battery hybrid power source," *Energy,* vol. 36, pp. 6490-6507, 2011.
5. R. Azizipanah-Abarghooee, T. Niknam, M. Zare, and M. Gharibzadeh, "Multi-objective short-term scheduling of thermoelectric power systems using a novel multi-objective θ-improved cuckoo optimisation algorithm," *IET Generation, Transmission & Distribution,* vol. 8, pp. 873-894, 2014.
6. M. Zaman, S. M. Elsayed, T. Ray, and R. A. Sarker, "Evolutionary algorithms for dynamic economic dispatch problems," *IEEE Transactions on Power Systems,* vol. 31, pp. 1486-1495, 2016.
7. L. B. Jaramillo and A. Weidlich, "Optimal microgrid scheduling with peak load reduction involving an electrolyzer and flexible loads," *Applied Energy,* vol. 169, pp. 857-865, 2016.
8. C. D. Korkas, S. Baldi, I. Michailidis, and E. B. Kosmatopoulos, "Intelligent energy and thermal comfort management in grid-connected microgrids with heterogeneous occupancy schedule," *Applied Energy,* vol. 149, pp. 194-203, 2015.
9. F. A. Mohamed and H. N. Koivo, "Multiobjective optimization using Mesh Adaptive Direct Search for power dispatch problem of microgrid," *International Journal of Electrical Power & Energy Systems,* vol. 42, pp. 728-735, 2012.
10. T. Niknam, R. Azizipanah-Abarghooee, and M. R. Narimani, "An efficient scenario-based stochastic programming framework for multi-objective optimal micro-grid operation," *Applied Energy,* vol. 99, pp. 455-470, 2012.
11. A. Kavousi-Fard, A. Abunasri, A. Zare, and R. Hoseinzadeh, "Impact of plug-in hybrid electric vehicles charging demand on the optimal energy management of renewable micro-grids," *Energy,* vol. 78, pp. 904-915, 2014.
12. M. Motevasel, A. R. Seifi, and T. Niknam, "Multi-objective energy management of CHP (combined heat and power)-based micro-grid," *Energy,* vol. 51, pp. 123-136, 2013.
13. M. Motevasel and A. R. Seifi, "Expert energy management of a micro-grid considering wind energy uncertainty," *Energy Conversion and Management,* vol. 83, pp. 58-72, 2014.
14. A. Baziar and A. Kavousi-Fard, "Considering uncertainty in the optimal energy management of renewable micro-grids including storage devices," *Renewable Energy,* vol. 59, pp. 158-166, 2013.
15. M. Hemmati, N. Amjady, and M. Ehsan, "System modeling and optimization for islanded micro-grid using multi-cross learning-based chaotic differential evolution algorithm," *International Journal of Electrical Power & Energy Systems,* vol. 56, pp. 349-360, 2014.
16. G. Aghajani, H. Shayanfar, and H. Shayeghi, "Presenting a multi-objective generation scheduling model for pricing demand response rate in micro-grid energy management," *Energy Conversion and Management,* vol. 106, pp. 308-321, 2015.

17. J. Soares, M. Silva, T. Sousa, Z. Vale, and H. Morais, "Distributed energy resource short-term scheduling using Signaled Particle Swarm Optimization," *Energy*, vol. 42, pp. 466-476, 2012.
18. J. Zhang, Y. Wu, Y. Guo, B. Wang, H. Wang, and H. Liu, "A hybrid harmony search algorithm with differential evolution for day-ahead scheduling problem of a microgrid with consideration of power flow constraints," *Applied energy*, vol. 183, pp. 791-804, 2016.
19. M. Elsied, A. Oukaour, T. Youssef, H. Gualous, and O. Mohammed, "An advanced real time energy management system for microgrids," *Energy*, vol. 114, pp. 742-752, 2016.
20. M. Marzband, M. Ghadimi, A. Sumper, and J. L. Domínguez-García, "Experimental validation of a real-time energy management system using multi-period gravitational search algorithm for microgrids in islanded mode," *Applied energy*, vol. 128, pp. 164-174, 2014.
21. J. Soares, M. A. F. Ghazvini, Z. Vale, and P. de Moura Oliveira, "A multi-objective model for the day-ahead energy resource scheduling of a smart grid with high penetration of sensitive loads," *Applied Energy*, vol. 162, pp. 1074-1088, 2016.
22. J. Sachs and O. Sawodny, "Multi-objective three stage design optimization for island microgrids," *Applied Energy*, vol. 165, pp. 789-800, 2016.
23. Y. Li, B. Feng, G. Li, J. Qi, D. Zhao, and Y. Mu, "Optimal distributed generation planning in active distribution networks considering integration of energy storage," *Applied Energy*, 2017.
24. J. Aghaei and M.-I. Alizadeh, "Multi-objective self-scheduling of CHP (combined heat and power)-based microgrids considering demand response programs and ESSs (energy storage systems)," *Energy*, vol. 55, pp. 1044-1054, 2013.
25. A. Chaouachi, R. M. Kamel, R. Andoulsi, and K. Nagasaka, "Multiobjective intelligent energy management for a microgrid," *IEEE Transactions on Industrial Electronics*, vol. 60, pp. 1688-1699, 2013.
26. M. Nemati, M. Braun, and S. Tenbohlen, "Optimization of unit commitment and economic dispatch in microgrids based on genetic algorithm and mixed integer linear programming," *Applied Energy*, 2017.
27. R. Alcorn and D. O'Sullivan, Electrical design for ocean wave and tidal energy systems: The Institution of Engineering and Technology, 2013.
28. S. Benelghali, M. E. H. Benbouzid, and J. F. Charpentier, "Generator systems for marine current turbine applications: A comparative study," *IEEE Journal of Oceanic Engineering*, vol. 37, pp. 554-563, 2012.
29. S. B. Elghali, M. Benbouzid, and J. F. Charpentier, "Marine tidal current electric power generation technology: State of the art and current status," in *Electric Machines & Drives Conference, 2007. IEMDC'07. IEEE International*, 2007, pp. 1407-1412.
30. M. Liu, W. Li, C. Wang, R. Billinton, and J. Yu, "Reliability evaluation of a tidal power generation system considering tidal current speeds," *IEEE Transactions on Power Systems*, vol. 31, pp. 3179-3188, 2016.
31. L. Mingjun, L. Wenyuan, Y. Juan, R. Zhouyang, and X. Ruilin, "Reliability evaluation of tidal and wind power generation system with battery energy storage," *Journal of Modern Power Systems and Clean Energy*, vol. 4, pp. 636-647, 2016
32. A. Askarzadeh, "Bird mating optimizer: an optimization algorithm inspired by bird mating strategies," *Communications in Nonlinear Science and Numerical Simulation*, vol. 19, pp. 1213-1228, 2014.
33. S. y. Obara, M. Kawai, O. Kawae, and Y. Morizane, "Operational planning of an independent microgrid containing tidal power generators, SOFCs, and photovoltaics," *Applied energy*, vol. 102, pp. 1343-1357, 2013.
34. Y. S. Lim and S. L. Koh, "Analytical assessments on the potential of harnessing tidal currents for electricity generation in Malaysia," *Renewable Energy*, vol. 35, pp. 1024-1032, 2010.
35. A. Etemadi, Y. Emami, O. AsefAfshar, and A. Emdadi, "Electricity generation by the tidal barrages," *Energy Procedia*, vol. 12, pp. 928-935, 2011.
36. Homepage of International Renewable Energy Agency, *IRENA Ocean Energy Technology Brief 3* www.irena.org/documentdownloads/publications/tidal_energy_v4_web.pdf, June 2014.
37. M. Sánchez, G. Iglesias, R. Carballo, and J. A. Fraguela, "Power peaks against installed capacity in tidal stream energy," *IET Renewable Power Generation*, vol. 7, pp. 246-253, 2013.
38. M. Khan, G. Bhuyan, M. Iqbal, and J. Quaicoe, "Hydrokinetic energy conversion systems and assessment of horizontal and vertical axis turbines for river and tidal applications: A technology status review," *Applied energy*, vol. 86, pp. 1823-1835, 2009.

39. S. Boronowski, K. Monahan, and G. C. van Kooten, "The Economics of Tidal Stream Power," in *2008 International Congress, August 26-29, 2008, Ghent, Belgium*, 2008.
40. M. B. Walsh, "Rising Tide in Renewable Energy: The Future of Tidal In-Stream Energy Conversion (TISEC), A," *Vill. Envtl. LJ*, vol. 19, p. 193, 2008.
41. G. Allan, M. Gilmartin, P. McGregor, and K. Swales, "Levelised costs of Wave and Tidal energy in the UK: Cost competitiveness and the importance of "banded" Renewables Obligation Certificates," *Energy Policy*, vol. 39, pp. 23-39, 2011.
42. A. Deihimi, B. K. Zahed, and R. Iravani, "An interactive operation management of a micro-grid with multiple distributed generations using multi-objective uniform water cycle algorithm," *Energy*, vol. 106, pp. 482-509, 2016.
43. D. Dallinger, *Plug-in electric vehicles integrating fluctuating renewable electricity* vol. 20: kassel university press GmbH, 2013.
44. W.-Y. Chang, "The state of charge estimating methods for battery: A review," *ISRN Applied Mathematics*, vol. 2013, 2013.
45. S. A. Alavi, A. Ahmadian, and M. Aliakbar-Golkar, "Optimal probabilistic energy management in a typical micro-grid based-on robust optimization and point estimate method," *Energy Conversion and Management*, vol. 95, pp. 314-325, 2015
46. S. Bandyopadhyay, U. Maulik, and A. Mukhopadhyay, "Multiobjective genetic clustering for pixel classification in remote sensing imagery," *IEEE Transactions on Geoscience and Remote Sensing*, vol. 45, pp. 1506-1511, 2007.
47. M. Gong, M. Zhang, and Y. Yuan, "Unsupervised Band Selection Based on Evolutionary Multiobjective Optimization for Hyperspectral Images," *IEEE Transactions on Geoscience and Remote Sensing*, vol. 54, pp. 544-557, 2016.
48. S. Rajasomashekar and P. Aravindhababu, "Biogeography based optimization technique for best compromise solution of economic emission dispatch," *Swarm and Evolutionary Computation*, vol. 7, pp. 47-57, 2012.
49. S. Sharma, S. Bhattacharjee, and A. Bhattacharya, "Grey wolf optimisation for optimal sizing of battery energy storage device to minimise operation cost of microgrid," *IET Generation, Transmission & Distribution*, vol. 10, pp. 625-637, 2016.
50. C. A. C. Coello, G. T. Pulido, and M. S. Lechuga, "Handling multiple objectives with particle swarm optimization," *IEEE Transactions on evolutionary computation*, vol. 8, pp. 256-279, 2004.